A role for Hho1p, a histone H1 homologue, in *Saccharomyces cerevisiae.*

Claudette Coert

SUBMITTED IN FULFILLMENT OF THE
REQUIREMENTS FOR THE DEGREE OF

MASTER OF SCIENCE

IN THE DEPARTMENT OF MOLECULAR AND CELL BIOLOGY
FACULTY OF SCIENCE
UNIVERSITY OF CAPE TOWN

2002

CONTENTS

ABBREVIATIONS

°C	Degrees celsius
Å	angstrom
ADP	Adenosine diphosphate
ATP	Adenosine triphosphate
AT-rich	DNA rich in adenine and thymine
bp	base pair
cdc 2	Cell-cycle dependent cyclin 2
cm	centimeter
Cs^-	Cold-sensitive
C-terminus	Carboxy terminus
Da	Dalton
DNA	Deoxyribonucleic acid
DNase I	Deoxyribonuclease I
E. coli	*Escherichia coli*
EDTA	Ethylene-diamene-tetra-acetic acid
g	gram or gravity constant
G1 phase	Gap phase 1
GC-rich	DNA rich in guanine and cytosine
h	hour
H1-GFP	H1 fused to Green Flourescent Protein
H1t	Testes specific H1
H_2O	water
His	L-Histidine

His-tag	Carboxy-terminal tract of 6 consecutive histidine residues
HNF3	Hepatocyte nuclear factor 3γ
IMAC	Immobilised Metal Affinity Chromatography
IPTG	isopropyl-β-D-thiogalactoside
kb	kilobases
kDa	kilodalton
LB	Luria Broth
MALDI-TOF	Matrix Assisted Laser Desorption Ionisation/ Time Of Flight
mg	milligram
min	minute
µg	microgram
µm	micrometre
µM	micromolar
µmol	micromole
mm	millimetre
mM	millimolar
mmol	millimole
mol	mole
MS	Mass Spectrometry
nm	nanometre
N-terminus	Amino-terminus
OD_{600}	Optical Density at 600 nm
ORF	Open Reading Frame
PCR	Polymerase Chain Reaction
RNA	Ribonucleic acid

mRNA	Messenger ribonucleic acid
rHho1p	recombinant Hho1 protein
rRNA	Ribosomal ribonucleic acid
rpm	Revolutions per minute
s	second (unit of time)
SDS	sodium dodecyl sulphate
SDS-PAGE	sodium dodecyl sulphate polyacrylamide gel electrophoresis
S-phase	Synthesis Phase
TFA	Triflouroacetic acid
Tris	Tris(hydroxymethyl)aminomethane
U	unit
Ura	L-Uracil
UV	Ultraviolet
V	Volt
v/v	volume per volume
w/v	weight per volume

ABSTRACT

It is well established that histone H1 is involved in facilitating the higher-order structures of chromatin. It has not become possible to test the biochemical function of H1 in *Saccharomyces cerevisiae*, since the identification of a H1 homologue (Landsman, 1996) with properties of a *bona fide* linker histone (Patterton et al., 1998; Ali, 2000). Such studies were difficult since no phenotype for a *HHO1* deleted strain has been published. In this study I have investigated the response of an *HHO1* disrupted strain to numerous conditions including UV radiation, osmotic and oxidative stress, γ-irradiation and longevity. It was found that *hho1*$^-$ cells were more sensitive to γ-irradiation, suggesting that the yeast cell accumulated more DNA double-strand breaks in the absence of H1, or the DNA repair pathways are responsive to chromatin structures in which H1 is involved. An additional phenotype that was identified in this study was an extended lag phase in *hho1*$^-$ strains when stationary phase cultures were exposed to 4°C. The misregulation of genes in the absence of H1 that are responsible for the appearance of this phenotype was investigated by microarray analysis. No specific class of gene was preferentially affected by the absence of H1. Very few differences in expression profile was seen before the lag phase or after 1h in the lag phase. Significantly, genes that are affected at the start of the lag phase were found to be clustered. The presence of these clustered regions on chromosome IV and VII suggest that regions of localised chromatin structure exist that enables genes to be activates quickly when they exit from stationary phase.

LIST OF FIGURES

LIST OF TABLES

ACKNOWLEDGEMENTS

I would like to extend my gratitude to my supervisor, Hugh Patterton, for his enthusiasm for science, and his continuous help throughout this project. Many thanks to Sari Pennings for hosting me during my overseas stint at the University of Edinburgh, and for the many stimulating discussions and helpful advice. I wish to thank Elize Muller-Patterton for the yeast strains, Dewald van Dyk for help with the microarray analyses, Anke Fiedler for help with the MALDI-TOF analyses, the Institute for Wine Biotechnology (University of Stellenbosch) for the use of the micromanipulator, and ARC-Infruitec for the use of the Co^{60}point-source. Thank you too, to Alastair Fleming and Kirrily Peters for helpful advice, and to the past members of the Patterton lab for showing me the ropes and keeping me sane. I would like to acknowledge the Wellcome Trust and UCT/EDP Molecular Biology Fellowship for funding. I wish to thank my family for encouraging me to take the leap into post-graduate study and for always supporting me. Lastly, I would like to thank Simon Boa for being my dearest friend in the laboratory, in the outdoors, and in the big wide world.

CHAPTER 1: INTRODUCTION

1.1 Chromatin

Chromatin is the term used to describe packaged DNA in a eukaryote nucleus. The fundamental structural unit of condensed chromatin is the nucleosome, which consists of 168 bp of DNA (Simpson, 1978), wrapped onto a histone octamer and associated at its ends with one molecule of linker histone (van Holde *et al.*, 1975). Adjacent nucleosomes are connected by a length of linker DNA. In 1974, Kornberg proposed a model explaining how the histones proteins interacted with each other and with the underlying DNA (Kornberg *et al.*, 1974). This model was adjusted slightly to include the linker histone (van Holde *et al.*, 1975).

1.2 Histones

The histones are a family of basic proteins involved in organising the DNA in the nuclei of eukaryotic cells. There are 5 major classes of histones, the core histones H2A, H2B, H3, and H4 and the linker histone H1 (reviewed in Wolffe, 1998). The histone octamer consists of two molecules of each of the core histones (Figure 1.1). Two molecules of histones H3 and H4 associate as a tetramer, to which two H2A-H2B heterodimers bind. Histone H1 binds to DNA at the terminal helical turn of the nucleosomal DNA, and at a position close to the pseudo-dyad axis (Zhou *et al.*, 1998; reviewed by Kornberg and Lorch, 1999).

Not all eukaryotic cells, however, utilise histones for packaging their DNA. Dinoflagellates package their DNA in small basic proteins completely unlike histones

(Vernet *et al.*, 1990), while in most mammalian species, the DNA in spermatozoa is compacted by basic proteins known as protamines (Poccia, 1986).

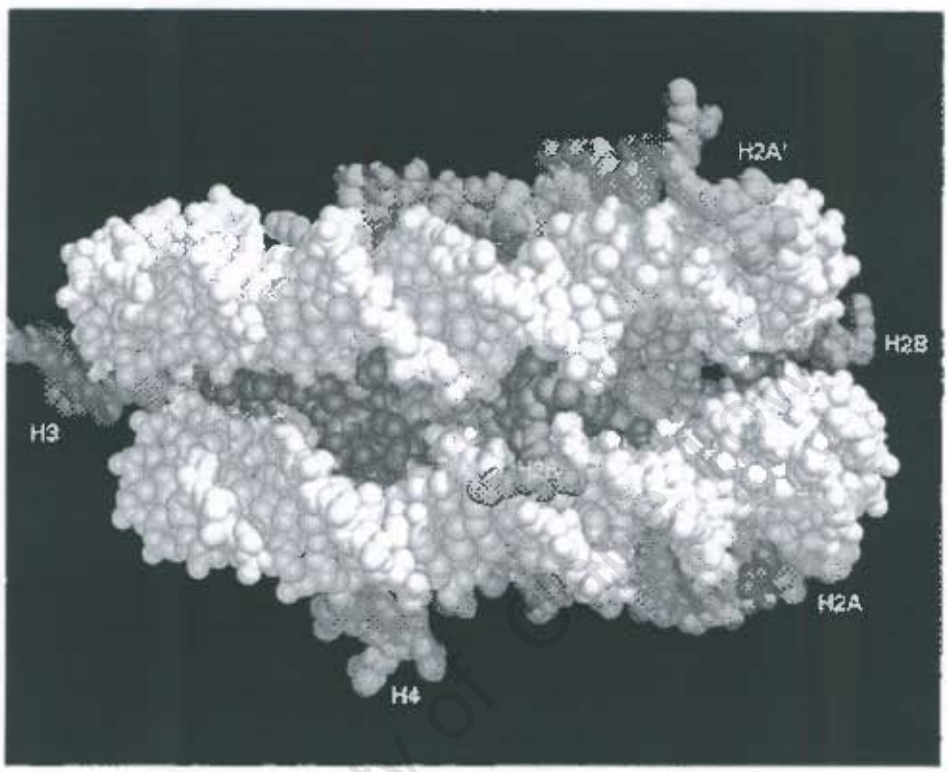

Figure 1.1Space-filling nucleosome model of the nucleosome
(taken from Luger et al., 1997: Crystal structure of the nucleosome core particle at 2.8 Å resolution)
The H2B (red) and H3 (blue) N-terminal tails pass through channels in the DNA superhelix (white) formed by aligned minor grooves. The other histones, H2A (yellow) and H4 (green) are indicated.

1.3 The Core Histones

The core histones are small basic proteins containing high molar percentages of lysine and arginine (van Holde, 1988). In the histone octamer these form a left-handed protein superhelix matching that of the DNA in the core particle (Klug *et al.*, 1980). The $[H3\text{-}H4]_2$ tetramer lies at the centre of this superhelix, with an H2A-H2B dimer at either end of the path.

The core histones all assume a similar structure with a basic N-terminal tail, a globular domain organised as a histone fold, and a C-terminal tail. The central C-terminal histone-fold domains of the core histones possess a high level of structural homology. The domain is formed through the interaction of three α-helices connected by two loops, which forms a crescent shaped hetero-dimer through the interaction of H3 and H4, and also H2A and H2B. Three α-helices linked by two loops form a histone fold. The interaction of two histone folds generates a handshake motif between two different histone proteins. The histone fold domains of the four core histones mediate histone-histone and histone-DNA interactions (Luger *et al.*, 1997).

The unstructured amino termini of the histones, consisting of 15-30 residues, are referred to as the histone tails. The N-terminal tail regions of H3 and H2B have random coil segments that pass between the gyres of the DNA superhelix. The N-terminal domain of H2A passes over the DNA along a minor groove. The amino acid base interaction within this groove may be important in modulating the nucleosomal association with particular DNA sequences. The H4 N-terminal tails appear to form divergent structures (Luger *et al.*, 1997), though this might be a limitation of the crystallisation techniques used to visualise the histones.

The histone tails are subjected to various post-translational modifications (Grunstein, 1997), including methylation, phosphorylation, acetylation, ADP-ribosylation, glycosylation and ubiquitination, which may modulate chromatin structure and serve as signals for interactions with other proteins (Strahl and Allis, 2000). Core histones are highly conserved between species ranging from yeast to human (De Lange *et al.*, 1969).

1.4 The Linker Histones (H1)

Linker histones are less conserved when compared to core histones, and tissue-specific subtypes of H1 are present in many organisms. An example is the chicken erythrocyte-specific linker histone, H5, the object of many chromatin studies.

Trypsin studies (reviewed by Bohm and Crane-Robinson, 1984) revealed that H1 had a tripartite structure, consisting of a central globular core and lysine rich N- and C-terminal domains (tails). The globular domain is made up of 3 α-helices terminating in a 3-stranded β-sheet (Ramakrishnan *et al.*, 1993). The globular domain binds to one DNA strand as it enters or exits the nucleosome, and to nucleosomal DNA near the dyad axis of symmetry of the nucleosome (Zhou *et al.*, 1998). The two proposed DNA-binding sites have been identified in the globular domain of the linker histone, and both were required for the appearance of a chromatosome stop with micrococcal nuclease digestion, which may indicate a requirement for correct positioning on the nucleosome (Goytisolo *et al.*, 1996). The highly basic linker histone tails partially neutralise negative charges on linker DNA (Clark and Kimura, 1990) and interact with DNA between nucleosomes.

Not all histone H1 histone family exhibit a tripartite structure. The ciliated protozoan *Tetrahymena* lacks the central globular domain (Wu *et al.*, 1986), while the yeast *Saccharomyces cerevisiae*, contains two globular domains separated by a lysine-rich linker region (Ushinksy *et al.*, 1996).

Linker histones exhibit a binding preference for supercoiled, rather than relaxed DNA, as well as for AT-rich regions (Wolffe and Brown, 1987). It is generally

accepted that H1 binds less tightly than other histones to DNA in chromatin (Wu *et al.*, 1986) and can readily exchange in living cells (Thomas and Rees, 1983). Exchange of histone H1 is rapid in both condensed and decondensed chromatin and occurs throughout the cell cycle (Lever *et al.*, 2000). Modulation of H1 binding is thought to be an important step for allowing the chromatin structure to change to facilitate transcription (Shen and Gorovsky, 1996). Using H1-GFP fusion proteins, Lever and colleagues (Lever *et al.*, 2000), have shown that H1-GFP was exchanged continuously between chromatin regions in living cells, with an average residence time of several minutes in both euchromatin and heterochromatin. Similarly, Misteli and colleagues (Misteli *et al.*, 2000) have shown, using an H1-GFP, that linker histones bind dynamically to chromatin in a human cell line. After hyperacetylation of core histones, the residence time of H1-GFP was reduced, which suggested a higher rate of exchange upon core histone modification. The dynamic nature of H1 binding is an essential feature of linker histones in their functions as regulators of chromatin remodelling and chromatin structure *in vivo*.

1.5 Linker Histone Modifications

The major post-translational modification of histone H1 involves cdc2 kinase catalysed phosphorylation at multiple sites. Serine and threonine residues are targeted on the N-terminal and C-terminal domains (Spencer and Davie, 1999).

The mechanism by which H1 phosphorylation affects transcription was investigated (Dou and Gorovsky, 2000). *Tetrahymena* strains were created with mutations in H1 that mimicked the charge of the phosphorylated region, without mimicking structure or hydrophillicity of the phosphorylated residues. It was found that a charge patch

occurs on the H1 molecule, which interacts with DNA. Interestingly, the charge patch is not restricted to a particular site, and can be dispersed throughout the H1 molecule (Dou and Gorovsky, 2002). Phosphorylation of H1 acts by changing the overall charge of a small domain. When this charge is affected by phosphorylation, decondensation of the chromatin fibre occurs. It has been shown to directly weaken the interaction of the basic tails of H1 with DNA, which disrupts the binding of the linker histone to chromatin, possibly destabilising the chromatin fibre (Hill *et al.*, 1991).

Phosphorylation acts as a first step mechanism to promote transient chromatin decondensation, which allows access to specific DNA binding factors (Thomas, 2000). These proteins may control DNA packaging and/or functional activities (Roth and Allis, 1992). Thus phosphorylation of H1 provides a means to initiate the process of chromatin remodelling in preparation for elevated levels in gene expression that occur as the cell responds to external signals or progresses through cell cycle regulated processes like gene activation, DNA replication and chromosome condensation (Lu *et al.*, 1998). *In vivo* experiments with temperature sensitive mutants defective in histone H1 phosphorylation, have shown that the decrease in H1 phosphorylation results in incomplete DNA replication (Lohr and Gross, 1993). Phosphorylation is cell-cycle dependent with the highest level of phosphorylation occuring at metaphase during mitosis, which is when the chromosomes are most condensed. This has led to the argument that a causal relationship exists between histone H1 phosphorylation and chromatin compaction (Bradbury *et al.*, 1974; Bradbury, 1992). Interphase phosphorylation of histone H1 is correlated with the

transcriptionally active states of chromatin (Roth and Allis, 1992; Lee and Archer, 1998).

There are currently two models explaining the role of H1 phosphorylation in chromatin condensation. In the model proposed by Bradbury and colleagues (Bradbury, 1992) explaining the role of H1 in chromosome condensation, non-phosphorylated H1 is present in decondensed chromatin, during interphase. H1 is loosely bound to DNA through interactions involving amino-terminal and carboxy-terminal tails, as well as the central globular domain. Upon phosphorylation of the H1 tails, the H1-DNA interactions are proposed to weaken, making way for H1-H1 interactions, which enables the formation of higher order chromatin structures (Figure 1.2a).

In the Roth and Allis model of 1992 (Figure 1.2b), the negative charge from linker DNA phosphates is shielded in condensed chromatin by the positively charged, non-phosphorylated tails of H1. Phosphorylation of the H1 tails increases the negative charge in the H1 molecule, thereby weakening H1-DNA interactions and causing a repulsion of adjacent fibres and the subsequent decondensation of chromatin. This ties in with the idea that chromatin folding *in vitro* is largely electrostatic in nature and is governed by repulsion between DNA regions that are reduced upon H1 binding. This decondensation might enable other proteins (eg. HMG proteins), involved in higher order DNA condensation, to interact with the DNA fibre, thereby facilitating mitotic chromatin condensation.

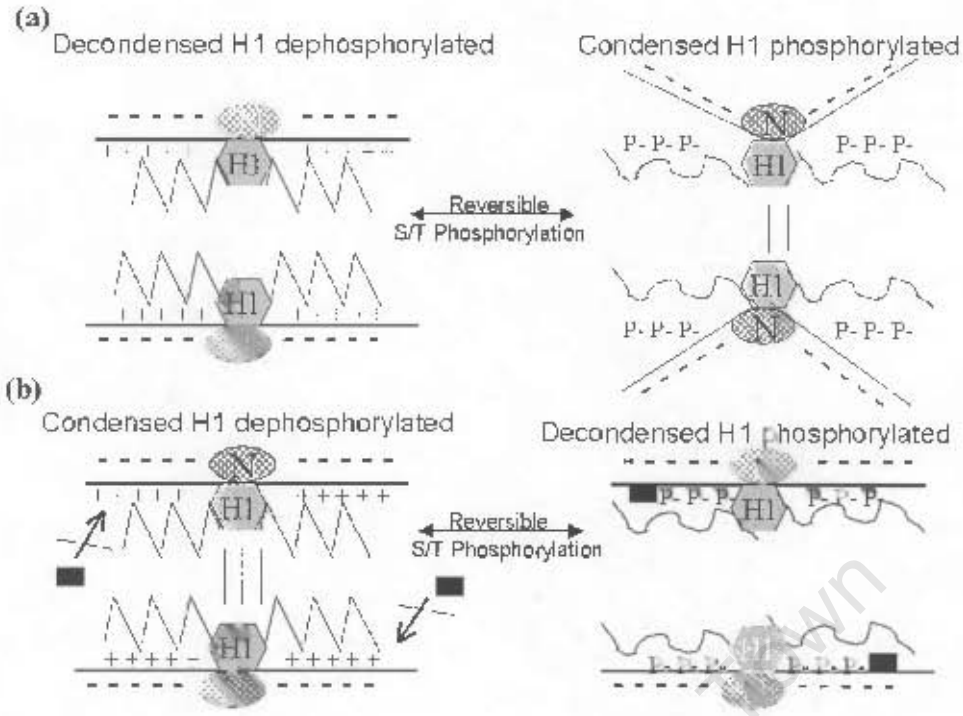

Figure 1.2 Models for the involvement of H1 phosphorylation in chromatin condensation. a) Bradbury model, 1974. Dephosphorylated H1 has a stronger interaction with DNA than with other HIs, favouring decondensation of chromatin. Once phosphorylated, H1 becomes less tightly bound to DNA, and favours H1-H1 interactions instead. Interactions between H1 molecules cause chromatin condensation. b) Roth/Allis model, 1992. Positive charge of the lysine rich tails of H1 enables chromatin condensation. Phosphorylation causes an increased negative charge of the H1 tails, and repulsion of the chromatin fibres, resulting in decondensation. Adapted from Roth and Allis, 1992.

Several studies have shown an involvement of linker histone phosphorylation in gene transcriptional activation (reviewed in Spencer and Davie, 1999). H1 phosphorylation is essential for rapid gene activation of the mouse mammary tumor virus (MMTV) long terminal repeat promoter by the glucocorticoid receptor in response to hormone binding (Lee and Archer, 1998). In the absence of glucocorticoid, the MMTV promoter is incorporated into six regularly positioned nucleosomes (Richard-Foy and Hager, 1987). This closed chromatin structure prevents the binding of activators to the promoter, thus inhibiting transcription (Archer *et al.*, 1992). Glucocorticoid exposure rapidly disrupts the local chromatin structure, recruiting transcription factors and inducing activation of the gene (Lee and Archer, 1994). Phosphorylation of the H1

tails is a prerequisite for the partial H1 loss and nucleosome disruption at this promoter. The promoter is silenced by the dephosphorylation of histone H1.

Mouse H1b phosphorylation is dependent upon ongoing transcription and replication processes (Davie and Chadee, 1998). This modification is unique in its dependence on transcription and replication. Studies on phosphorylation in *Tetrahymena* show that this modification mimics the loss of H1 from chromatin (Dou and Gorovsky, 2000). Phosphorylation of macronuclear H1 is also not essential for viability (Mizzen *et al.*, 1999).

A lesser characterised modification of H1 is ubiquitination. $TAF_{II}250$ not only has acetyltransferase activity, but also has histone-ubiquitination activity (Pham and Sauer, 2000). Drosophila $TAF_{II}250$ can mediate the mono-ubiquitination of histone H1 *in vitro*. Since $TAF_{II}250$ is recruited to promoters, ubiquitination of histone H1 in eukaryotes may regulate chromosomal gene activity in a promoter specific manner (Wu and Grunstein, 2000).

1.6 The Functions of Histone H1

1.6.1 The Function of H1 in Repression

Histone H1 was initially thought to be a general repressor that ensured a strong and stable repression of tissue specific genes (Weintraub, 1985). This was based on the premise that gene repression may be dominated by the higher order structure of nucleosomes and that H1 was involved in the formation and maintenance of these structures. In eukaryotes, transcriptional repression correlates in general with chromatin condensation. This can be either domain-wide or local, encompassing, in

the latter case, just a few nucleosomes (Travers, 1999). During transcriptional repression, linker histones may also prevent access of transcription factors and chromatin remodelling complexes to DNA (Strahl and Allis, 2000).

Histone H1 selectively represses the transcription of genes during *Xenopus* development. *In vitro* the incorporation of histone H1 into chromatin can repress the transcription of many genes including the *Xenopus* 5S rRNA gene (Nightingale and Wolffe, 1995). The two 5S rRNA multigene families of *Xenopus* provide an example of selective repression by H1. The expression of both the somatic and oocyte rRNA genes is developmentally regulated, and the selective repression of the oocyte 5S rRNA coincides with the onset of H1 expression without affecting the transcription of somatic 5S rRNAs (Schlissel and Brown, 1984). The somatic 5S rRNA genes (400 copies per haploid genome) are active in both somatic and oocyte cells, whereas the oocyte 5S rRNA genes (20,000 copies) are only transcribed in oocytes (Wormington and Brown, 1983). The two types of genes have virtually identical coding sequences but differ in the sequence of their flanking DNAs – that of the somatic genes is GC rich, while that of the oocyte genes is AT rich (Peterson *et al.*, 1980). Transcriptional activation of the two genes require the same set of transcription factors and the primary event in the formation of the transcription complex, is the binding of TFIIIA to the internal control region (Engelke *et al.*, 1980).

There are currently two models explaining why the somatic genes are active in both oocyte and somatic cells. In the model proposed by Wolffe and colleagues (Vermaak *et al.*, 1998), the 5S rRNA is occluded from the transcriptional machinery because histone H1 positions the nucleosome in the oocytes. In somatic 5S rRNA genes

nucleosome positioning occurs, so the essential promoter elements are accessible and the genes are therefore transcriptionally competent. Therefore, H1 organises the chromatin, affecting transcriptional activity in a nucleosomal context (Sera and Wolffe, 1998). Alternately, in the 1998 model of Rhodes and colleagues (Panetta *et al.*, 1998), TFIIIA binds more efficiently to nucleosomes containing somatic 5S rRNA than to nucleosomes on oocyte 5S rRNA genes, as a result of differences in the nucleosome positions on the respective genes.

1.6.2 The Role of H1 in the Cell Cycle

Linker histones have a defined role during the cell cycle. Linker histone levels are lowest at the start of S-phase, increasing progressively during the M and T-phases. The highest levels are reached during G1 phase followed by a sudden drop at the start of S-phase (reviewed in Roth and Allis, 1992; Spellman *et al.*, 1998).

In HeLa cells H1 dissociates from the DNA to a large extent during replication and chromosome condensation, but not in interphase when the cells are transcriptionally active (Bleher and Martin, 1998). During human diploid fibroblast differentiation the histone variant $H1^{\circ}$ is expressed as a function of the cell cycle. Increased $H1^{\circ}$ mRNA levels occur during the S-phase in actively proliferating cell cultures (Tsapali *et al.*, 2000).

1.6.3 The Structural Roles of H1

A variety of structural roles have been attributed to linker histones, including completion and locking of the two DNA turns within a nucleosome, determination of average nucleosome spacing, and facilitation of folding of the 10nm nucleosome-

containing fibre into higher order structures (Garrard, 1991; Zlatanova and Van Holde 1992). It is generally understood that linker histones play a critical role in maintaining the structure of the 30nm fibre (Thoma *et al.*, 1979; Allan *et al.*, 1981). It has also been suggested that linker histones play a role in levels of chromatin compaction beyond that found in the 30nm fibre (Weintraub, 1985). The globular domain of H1 and either the H1 tails or the H3 tail domains are needed to stabilise the 3-D arrangement of nucleosomes (Zlatanova *et al.*, 1998). In plants H1 subtypes often differ in amino acid sequence and in the length of the C-terminal tail, which affects the ability to mediate higher order chromatin structure (Cole, 1984).

The linker histone of the ciliated protozoan *Tetrahymena* lacks the globular domain of the linker histones in other species (Wu *et al.*, 1986). Strains without H1 grow at normal rates, and undergo normal mitosis, though the chromosome structure is less condensed. Therefore linker histones are not essential for cell survival, though they are involved in chromatin packaging and condensation *in vivo* in this organism (Shen *et al.*, 1995).

Vertebrate telomeres contain arrays of nucleosomes with unusually short and regular repeat lengths. Therefore telomeres are organised as specialised nucleosome arrays with features similar, but not identical, to bulk chromatin (Bedoyan *et al.*, 1996). Histone H1 has been shown to bind to dinucleosomes and not mono-nucleosomes in rat telomeres (Makarov *et al.*, 1993).

Transcription factors that share structural features with histones or HMG proteins function architecturally, remodelling DNA to facilitate the assembly of higher order

nucleo-protein structures that activate or repress transcription (Wolffe, 1994). HNF3, which contains a winged helix motif similar to that found in histone H1, can replace H1 in the chromatin of the mouse serum albumen enhancer (Cirillo *et al.*, 1998).

Alterations in chromatin structure resulting from changes in linker histone stoichiometry, may modulate the levels or rates of core histone acetylation *in vivo* (Gunjan *et al.*, 2001). Linker histones H1 and H5 (an H1 variant in chicken erythrocytes) specifically inhibit acetylation of mono- and oligo-nucleosomes. Linker histones hinder access to PCAF and other histone acetyltransferases to their target sites. Disruption of linker histone higher order compaction is a prerequisite for efficient acetylation of histone tails in nucleosomes (Herrera *et al.*, 1999). Chromatin fractions enriched in acetylated core histones have decreased levels of H1 (Davie and Nickel, 1987). Acetylation of core histones, which causes destabilisation of the chromatin fibre (Garcia-Ramirez *et al.*, 1995) might lead to increased dissociation of H1 (Perry and Annunziato, 1989). This strengthens the argument that H1 is a trigger for gene repression, since acetylation is a general activation signal.

Methylation studies on *Tetrahymena* show that methylation is preferential in linker DNA (Harrison *et al.*, 1986) but Karrer *et al* (2002) have shown recently that methylation patterns in linker DNA are unaffected by the presence or absence of H1.

1.6.4 The Role of H1 in Transcriptional Control

It is known that H1 is involved in the finer control of the transcriptional activity of individual genes (Zlatanova, 1990) and effects nucleosomal dynamics (Pennings et al., 1994). Inclusion of the linker histone into the nucleosome requires the presence of an octamer of core histones and restricts the translational mobility of histone octamers with respect to the associated DNA sequence. Binding of linker histones leads to the partial rearrangement of the core-histone interactions in the nucleosome (Lee and Hayes, 1997).

ATP-dependent multiprotein complexes use the energy of ATP hydrolysis to enhance the accessibility of nucleosomal DNA (Vignali, *et al.*, 2000). H1 incorporation causes a global inhibition in the binding of these complexes (e.g. ySWI/SNF and hSWI/SNF), which can be overcome by the phosphorylation of the linker histone (Aoyagi *et al.*, 2002). Nucleosomes containing H1 are remodelled more slowly than nucleosomes lacking H1. An example is hSWI/SNF where the chromatin remodelling activity is reduced on nucleosomes containing H1 (Hill and Imbalzano, 2000). Addition of H1 to the nucleosome forms a structure that is more resilient to the remodelling activity of hSWI/SNF.

1.6.5 The Role of H1 in Development

Linker histones can be subdivided into distinct classes according to where they are expressed during development in vertebrates (Khochbin and Wolffe, 1994).

In unfertilised sea-urchin oocytes during early embryogenesis the levels of cleavage-specific linker histones increase when a high rate of cell division is needed (Ohsumi

and Katagiri, 1991). However, when activation of zygotic expression occurs, common somatic H1s accumulate. This is followed by the accumulation of differentiation specific H1s and an arrest of cell proliferation during the formation of different tissues (Grunwald *et al.*, 1995). Therefore, during crucial periods in development e.g. sperm decondensation and mid-blastula transition, linker variants change in chromatin, thereby causing changes in gene expression (Dimitrov *et al.*, 1993; Bouvet *et al.*, 1994).

In *Xenopus* the type of histone H1 variant changes as the cell cycle lengthens (Brocard *et al.*, 1997). Eggs and embryos at stages before the mid-blastula transition are deficient in histone H1 and instead have an oocyte-specific variant called B4 (Newport and Kirschner, 1982). After the midblastula transition, histone B4 is progressively substituted by three somatic histone variants until the neurula stage is reached (Dimitrov *et al.*, 1993). Linker histone B4 binds to the nucleosomal core at much lower affinities than somatic histone variants, therefore embryonic chromatin is more dynamic. This facilitates the exceptionally rapid embryonic cell cycles (Ura *et al.*, 1994; Nightingale *et al.*, 1996; Ura *et al.*, 1996). Replacement of histone B4 *in vitro* with somatic linker histones fixes the position of nucleosomes on the DNA (Ura *et al.*, 1995). Chromatin compaction and higher order structure results (Wolffe, 1989).

H1 double knockouts in mice show no significant change in the ratio of total H1 to nucleosomes. In these mice $H1^{\circ}$ and either H1c, d or e were knocked out. This study showed that individual H1 subtypes are dispensable for mouse development and the loss of even two subtypes is tolerated if a normal H1-to-nucleosome stoichiometry is maintained (Fan *et al.*, 2001).

In the plant, *Arabidopsis*, three H1 variants occur (Ascenzi and Gantt, 1999). Two genes encoding for virtually identical mass histones, H1-1 and H1-2, are expressed in a wide variety of tissues and make up the majority of the linker histone species. However, Histone H1-3 is localized differently and does not bind to 5S rDNA sequences like the other variants do.

In the tobacco plant Prymakowska-Bosak and colleagues showed in 1996 that doubling the H1-DNA ratio in chromatin increased the level of chromatin condensation, however little effect on basal cellular functions were seen (Prymakowska-Bosak *et al.*, 1996). The same group showed that the native stoichiometry of linker histones was critical for the correct course of male meiosis and the development of functional pollen grains (Prymakowska-Bosak *et al.*, 1999).

1.6.6 Specialised Roles for H1

H1 seems to have specialised functions in certain organisms. In the tomato plant H1-S, a drought-induced H1 variant, accumulates in nuclei and chromatin of tomato leaves subjected to water deficit stress (Chao *et al.*, 1999; Scippa *et al.*, 2000). In this case H1-S seems to be induced as a stress-response. While in the fungus, *Ascobolus*, mutant strains lacking H1 have a decreased lifespan. Between six and thirteen days after germinating, they stop growing and display hypermethylation and increased MNase accessibility. Therefore, H1 is necessary for a long life span and chromatin condensation in *Ascobolus* (Barra *et al.*, 2000; reviewed by Ausio, 2000).

1.6.7 Is Histone H1 essential?

H1 is not essential for DNA compaction. In the absence of H1, the tails of H3 and H4 are required for the formation of the moderately folded chromatin conformation (Tse and Hansen, 1997). Therefore, H1 is not essential for chromatin folding, though its removal possibly destabilises both local and higher order chromatin structures, by altering core histone-DNA interactions (Usachenko, 1996; reviewed in Wolffe and Hayes, 1999).

The presence of physiological levels of linker histones is not needed to form a functional nucleus. Dasso and colleagues (Dasso *et al.*, 1994) showed that when H1 was depleted in *Xenopus* eggs, the nucleus was still functional. Furthermore, DNA binding proteins, have been shown to functionally complement the role of H1 in the absence of the linker histone. The levels of HMGB 1,2 proteins increase 2-fold in the absence of H1 in the DT40 chicken B cell line (Takamai and Nakayama, 1997), while HMG-D takes on the role of H1 when the linker histone is deleted in *Drosophila* (Ner and Travers, 1994).

The H1 variant, H1t, has a specialised role in spermatogenesis. Mice with a disrupted form of the H1t gene are still fertile and show no detectable defect in spermatogenesis even when they are homozygous for the defective gene. Other H1 subtypes seem to compensate for the loss of the H1t variant, therefore H1t is not essential for functional sperm production (Lin *et al.*, 2000).

The histone H1 gene, *HHOA*, in the fungus *Aspergillus* is a typical linker histone with one central globular domain. When deleted, no obvious phenotype is observed (Ramon *et al.*, 2000).

1.7 Histone H1 in *Saccharomyces cerevisiae* (*HHO1*)

No histone H1 has been isolated from yeast and it was long thought that there was no requirement for neutralisation of the linker DNA charge, since yeast possesses short repeat length chromatin with a ~166 bp repeat and a linker length of 0 bp (Reviewed by Thomas, 2000) In addition, a large component of the yeast genome is transcriptionally active compared to the genomes of higher organisms (Davie *et al.*, 1981). However, the possible presence of yeast H1 had been reported based on its immunological detection, using anti-mouse H1 antibodies (Srebreva *et al.*, 1987; Smith et al., 1984). The complete sequencing of the yeast genome in 1996 (Goffeau *et al.*, 1996), revealed an open reading frame encoding a candidate H1 (Hho1p), which was different to the normal tripartite H1 but had homology to the globular domain of known H1s in other organisms (Landsman, 1996; Ushinsky *et al.*, 1997). The *HHO1* gene, found on chromosome XVI between positions 308827 and 309603 in *S. cerevisiae*, was the only candidate gene to exhibit this homology. There is only one copy of this gene in the yeast genome (Ushinsky *et al.*, 1997).

HHO1 encodes a protein (Hho1p) 258 amino acids in length with a predicted molecular weight of ~ 28 kDa. Comparison of the protein sequence with itself revealed a second globular domain (Landsman, 1996). Hho1p is therefore structurally different from canonical H1s since it has two globular domains of about 80 residues, with a basic amino-terminal extension and a basic, lysine-rich linker region (38

residues) which connects the two globular domains (Figure 1.3). The linker region shows homology to the C-terminal tails of other histones, since it contains 12 lysines, 10 alanines and four prolines out of 42 residues (Landsman, 1996). The globular domains of Hho1p are not identical, and they might therefore have different functional roles. The predicted tertiary structure of Hho1p resembles the winged-helix structure of known H1s (Patterton *et al.*, 1998; Baxevanis and Landsman, 1998; Ali, 2001).

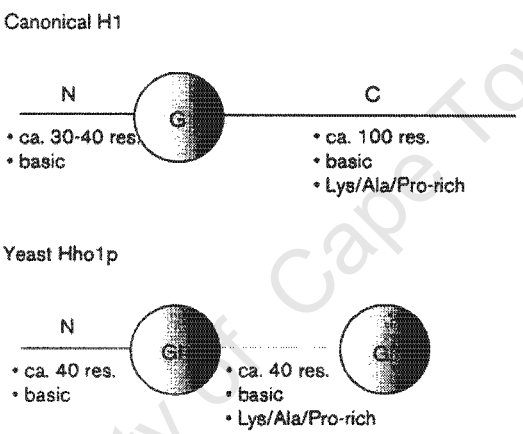

Figure 1.3 Comparison of the putative yeast H1 with the canonical H1.
Domain organisation. The two homologous domains (GI and GII) of Hho1 p, which are also homologous to the central globular domain (G) of a typical H1, are connected by a basic linker, which shows some similarity to the much longer carboxy-terminal basic domain (C) of H1. Both H1 and Hho1p have a basic amino-terminal domain (N). Courtesy of Thomas, 2000.

Using Hho1p-GFP fusion proteins, Hho1p has been shown to localise in the nucleus (Ushinsky *et al.*, 1997). These studies also confirm that Hho1p is in close proximity to DNA. Recombinant Hho1p displayed electrophoretic and chromatographic properties similar to that of the linker histones and forms a stable ternary complex with a reconstituted dinucleosome core *in vitro* with molar rHho1p: core histone ratios of up to 1 (Patterton *et al.*, 1998). Deletion of the *HHO1* gene has little effect on telomeric silencing, basal transcriptional repression, or gene activation at a distance and does not affect nucleosome repeat length (Patterton *et al.*, 1998; Escher and Schaffner,

1997). Furthermore, Hho1p is able to bind to four-way DNA junctions (Ali, 2001). Although Hho1p binds H1-depleted chromatin and protects an additional ~20 bp of DNA beyond the core particle length against exonuclease digestion (Patterton *et al.*, 1998), it is not clear whether the protein functions globally as a true H1, or whether it performs the role of H1 on a particular subset of genes in yeast.

HHO1 is transcribed throughout the cell cycle and its synthesis matches the expression pattern of the core histones, where a peak in transcription occurs during S-phase (Spellman *et al.*, 1998). Hellauer *et al* (Hellauer *et al.*, 2001) produced an *HHO1* deletion in WT yeast haploid cells. The deletion and wildtype strains were grown in rich medium and the RNA was isolated for microarray analysis on the entire genome. These results showed no significant increase in the expression of genes in *hho1*$^{-}$, but rather, a modest decrease in expression. These data therefore do not support the hypothesis that Hho1p is associated with the repression of transcription in yeast. These results were supported by a subsequent study (Freidkin and Katcoff , 2001).

Freidkin and Katcoff (Freidkin and Katcoff, 2001) detected a stoichiometry of one Hho1p molecule per 37 nucleosomes in WT cells. However, later studies by Ali and Thomas (Ali, 2001) showed that one molecule of Hho1p associates with every nucleosome. The binding mechanism of *HHO1* is also controversial. In the Freidkin and Katcoff study it was suggested, using chromatin immunoprecipitation studies that Hho1p binds preferentially to restricted locations in the yeast genome i.e. rDNA regions, while Ali and Thomas suggested that, like known linker histones, Hho1p is distributed throughout the genome.

1.8 Project Aims

This project is aimed at understanding the biological role of histone H1 in *Saccharomyces cerevisiae* as a model for the action of this chromatin-associated protein in higher eukaryotes.

The first aim was to purify Hho1p in sufficient amounts in order to generate an anti-serum against the protein (Chapter 3). The second aim was to develop a hypothesis about the functional and biological role of Hho1p, by investigating the reaction of *hho1*$^-$ to a host of stress conditions (Chapter 4). Finally, based on the determination of a probable phenotype, microarray studies were performed, to elucidate the difference in gene expression profiles at various points in growth (Chapter 5).

CHAPTER 2: MATERIALS AND METHODS

All chemicals used in this study were chemically pure grade and supplied by Merck, unless otherwise stated. Water had a specific resistance of 18.2Ω and was produced with a milli-Q apparatus (Milli-Pore). Primers were made by the in-house oligonucleotide synthesis facility. All reagents used were molecular biology grade and, unless stated otherwise, all standard molecular biology techniques were performed according to established protocols (Ausubel *et al.*, 1995 and Adams *et al.*, 1998).

2.1 Expression and Purification of Recombinant Hho1p (rHho1p)

2.1.1 Expression of Recombinant Hho1p (rHho1p)

Full-length recombinant yeast Hho1p was expressed from the plasmid pET20b (+)-*HHO1* (Patterton *et al.*, 1998) in *Escherichia coli* strain BL21(DE3) containing the T7 lysozyme producing plysS plasmid (Stratagene).

The optimal induction time for maximal protein yield was determined by conducting an induction time-course study. A single colony of BL21DE3 containing (pLysS), that was transformed with the pET20b (+)-*HHO1* construct, was inoculated into 10 mℓ of Luria-Bertani (LB) Broth medium (5 g/ℓ yeast extract, 5 g/ℓ sodium chloride, 10 g/ℓ tryptone, 1mM NaOH) supplemented with 50 µg/mℓ ampicillin and 30 µg/mℓ chloramphenicol. Cultures were grown at 37°C to an OD_{600} of 0.7. Isopropyl-1-thio-β-D-galactopyranoside (IPTG) was added to a final concentration of 0.4 mM and the cultures were returned to 37°C for agitated growth. Aliquots (1 mℓ) were taken at timed intervals (0, 30, 60, 120

and 180min), and the cells pelleted (13,200 × g, 10 s) in a microfuge. Each pellet was resuspended in 20 μℓ of 5 × SDS-PAGE sample application buffer (0.5 M Tris-Cl (pH 6.8), 10% (w/v) sodium dodecyl sulphate (SDS), 0.1% (w/v) bromophenol blue, 10% (v/v) glycerol) and 2% (v/v) β-mercaptoethanol was added. Samples were heat denatured at 95°C, cooled on ice and loaded onto 15% (w/v) polyacrylamide gels.

2.1.2 SDS-PAGE gel electrophoresis of proteins

All SDS-PAGE analyses of protein samples were performed using the Laemmli discontinuous method (Laemmli, 1970). Running gels consisted of 12% (w/v) polyacrylamide matrix (acrylamide:bisacrylamide, 29:1) in 375 mM Tris-Cl and 0.1% (w/v) sodium dodecyl sulphate (SDS), and were overlaid with a 6% (w/v) polyacrylamide stacking gel (acrylamide:bisacrylamide, 29:1) in 125 mM Tris-Cl and 0.1% SDS. Samples were denatured at 95°C in SDS sample application buffer (200 mM Tris-Cl (pH 6.8), 2% (w/v) SDS, 0.02% (w/v) bromophenol blue and 2% (v/v) glycerol), cooled on ice, and loaded onto the gel. Gels were electrophoresed at 150 V for 1h in a MiniProtean III (Bio-Rad Laboratories, Hercules, CA, USA) electrophoresis system, unless otherwise indicated. Following electrophoresis, gels were stained with Coomassie Blue stain solution for 1 h (0.25% (w/v) Coomassie Brilliant Blue in 25% (v/v) ethanol), and destained overnight in destain solution (7% acetic acid, 25% ethanol). Ethanol was substituted with methanol in the destain solution where protein samples were to be analysed by MALDI-TOF mass spectrometry.

2.1.3 Large-scale crude protein extraction

Large-scale purification of rHho1p was performed by inoculating a single colony of BL21DE3 (pLysS) containing the pET20b (+)-*HHO1* construct, into 5 mℓ LB supplemented with 50 μg/mℓ ampicillin and 30 μg/mℓ chloramphenicol, and grown at 37°C to an OD_{600} of 0.7. This pre-inoculum was added to 1ℓ LB, containing the same concentrations of ampicillin and chloramphenicol, and incubated at 37°C with continuous agitation until OD_{600} of 0.7 was reached. Cells were harvested by centrifugation (2000 × g, 5min, 4°C) in a JA14 rotor (Beckman). The cell pellet was resuspended in 1ℓ LB, containing ampicillin and chloramphenicol. IPTG was added to a final concentration of 0.4 mM and the cultures were returned to 37°C for agitated growth. It was previously shown that better protein yields were obtained by replacing the ampicillin-containing LB medium prior to induction, because expression of Hho1p is slightly toxic to *E. coli*, resulting in plasmid loss and lower protein yields under conditions where the antibiotic becomes depleted (Patterton *et al.*, 1998). Cells were harvested by centrifugation (2000 × g, 5min, 4°C) in a JA14 rotor, using the conditions described above, and resuspended in 10 mℓ binding buffer (5 mM imidazole, 500 mM NaCl, 20 mM Tris-Cl, pH 7.9). Cell lysis was carried out by sonication on a Bronwill Biosonik III sonicator (Bronwill Scientific, Inc., New York) at a maximum intensity setting using fifteen 30s pulse/ rest cycles. The sonicated lysates were centrifuged (38,500 × g, 20min, 4°C) in a JA20 rotor (Beckman). The supernatant was collected and used for subsequent purification.

2.1.4 Protein purification

Recombinant Hho1p was purified by metal-chelation chromatography using a His-Bind kit (Novagen). A 50% slurry of nickel agarose resin (2.5 mℓ) was packed into a plastic column (7 cm × 1 cm). The column was washed as follows: firstly, 7.5 mℓ H_2O was allowed to flow through under gravity, followed by 12.5 mℓ charge buffer (50 mM $NiSO_4$) and 7.5 mℓ of binding buffer. Crude protein extract (approximately 10 mℓ) was applied to the column. The column was washed with 25 mℓ of binding buffer and 15 mℓ wash buffer (40 mM imidazole, 500 mM NaCl, 20mM Tris-Cl, pH 7.9). Aliquots (1 mℓ) of each fraction were collected and stored at –20°C. Elution buffer (10 mℓ) containing 1 M imidazole, 0.5 M NaCl, 20 mM Tris-Cl (pH 7.9) was added and 1 mℓ fractions were collected. Fractions were stored at -20°C and 10 μℓ aliquots of each fraction (crude extract, binding wash, wash and elution fractions) were loaded on a 12% (w/v) SDS polyacrylamide gel cast in a Gibco BRL V15-17 Vertical Gel Electrophoresis Apparatus (Life Technologies, Gaithersburg, MD, USA) and electrophoresed at 200 V for 2 h. Proteins were visualised by Coomassie stain as described above. The identity of the protein in the band corresponding to rHho1p was verified by MALDI-TOF, as described below.

In order to purify rHho1p away from a contaminating acidic bacterial protein that bound to the Ni^{2+} column, fractions containing rHho1p were pooled, concentrated in a 10 kDa molecular weight cut-off (10 MWCO) Centrex Centrifugal Ultrafilter column (Schleicher and Schuell, Dassel, Germany), washed with 10mM sodium phosphate (pH 7.0), 0.5mM

phenylmethylsulfonyl fluoride (PMSF) and loaded onto a 1 mℓ bed-volume CM-Sephadex C25 cation exchange column, equilibrated with 10 mℓ of the sodium phosphate buffer. The column was developed with 10 mℓ of a 0 to 1000 mM linear gradient of NaCl in 10mM sodium phosphate (pH7.0), 0.5mM PMSF. Fractions (1 mℓ) were collected and loaded onto a 12% (w/v) SDS-PAGE gel and electrophoresed at 150 V for 1hour. Proteins were visualised by Coomassie stain as described above. Fractions containing rHho1p were concentrated using a 10 MWCO Centrex Centrifugal Ultrafilter column.

2.1.5 In-gel trypsin digest and MALDI-TOF analysis

Following SDS-PAGE electrophoresis and Coomassie Brilliant Blue Staining, gels were destained in 7% (v/v) acetic acid, 25% (v/v) methanol for 16 hours. Protein bands to be analysed were excised from the gel. The band corresponding to carbonic anhydrase in the Broad Range Molecular Marker (Bio-Rad Laboratories, Hercules, CA, USA), was also excised as a positive control, while a blank gel piece was excised as negative control. Each slice was washed twice with 200 μℓ 50% (v/v) acetonitrile, 25 mM NH_4HCO_3. A 15 min incubation period was allowed before removing the solution. Gel slices were washed once with 200 μℓ 100% (v/v) acetonitrile, and gel slices were dried in a rotary evaporator for 20-30 min. Trypsin (20 μℓ of 20 μg/mℓ, Sigma-Aldrich) and 25 mM NH_4HCO_3 was added, and the sample was incubated overnight at 37°C. Acetonitrile and TFA (50% (v/v) and 5% (v/v), respectively) were added to a final volume of approximately 70 μℓ, and samples were allowed to stand for 30 min. The liquid fraction was transferred to a fresh eppendorf tube and dried. Samples were dissolved in 60 μℓ

0.05% (v/v) TFA, 5% (v/v) acetonitrile and mixed in a 1:1 dilution with an α-cyano-4-hydroxycinnamic acid (10 mg/mℓ in 60% (v/v) acetonitrile, 0.3% (v/v) TFA) matrix. A 2 μℓ aliquot of this solution was spotted on a gold-plated grid. MALDI spectra were captured in the linear mode. Typically, analyses were performed at an accelerating voltage of 20 000 V and a grid voltage of 74 %, while the negative ion selector was switched off. The fragment sizes determined were analysed using the MS-Fit Program available at ***http://prospector.ucsf.edu***, and subjected to database searches to confirm the identity of the protein (Clauser *et al.*, 1999).

2.1.6 Preparation of polyclonal anti-serum to rHho1p

Two New Zealand rabbits were injected into the marginal vein of the ear with 1 mℓ antigen emulsion, comprised of 500 μℓ Freund's incomplete adjuvant (Ausubel *et al.*, 1995) and 500 μℓ (200μg) rHho1p. Subsequent injections were administered at 7, 14, 30 and 60 days. Blood samples were removed from the rabbits at 30 and 60 days. The rabbits were terminated after 90 days by ketamine-xylazine anaethetisation followed by exanguation.

2.2 Phenotypic Characterisation

2.2.1 Strains and reagents used

All phenotypic characterisations were performed using both W303 and FY2 background strains (wildtype) and their corresponding *HHO1* knockout strains, unless indicated otherwise. The W303-*hho1*$^-$ knockout strain was constructed in the laboratory, while the FY2-*hho1*$^-$ knockout strain was purchased (Research Genetics).

2.2.2 Yeast strains, media and growth conditions

S. cerevisiae strains that were used in this study were derived from W303 [MAT**a**, *leu 2-3, 112ura 3-1, trp 1-1, his 2-11, 15 ade 2-1, can 1-100, GALSUC1 mal0*] and FY2 [MATα, *ura 3-52*]. These yeast strains were a kind gift from the Institute for Wine Biotechnology, University of Stellenbosch. Yeast media were made as described previously (Adams et al., 1998). The rich medium (YPD) contained 1% (w/v) Bacto-yeast extract, 2% (w/v) Bacto-peptone (Difco) and 2% (w/v) glucose. The drop-out media contained 0.34% (w/v) Bacto-Yeast Nitrogen Base (without amino acids), supplemented with either histidine at 0.37 g/litre or uracil at 0.37g/litre (Bio 101) dropout media and 1M sorbitol. For plates, 2% (w/v) Bacto-agar was added before autoclaving. Yeast cultures were incubated at 30°C with agitation.

2.2.3 Construction of the *HHO1* knockout strain

Plasmid pRS413yH1-small-his3 (Patterton *et al.*, 1998) was isolated from *E. coli* strain SURE (Life Sciences) using the Wizard Maxiprep System (Promega), according to the manufacturers instructions. The plasmid DNA was eluted in water. 40 μℓ quantities of

electro-competent W303 S. cerevisiae cells (Guarente, 1991) were transformed by electroporation with 100 ng (in a volume of 5 μℓ) of the above plasmid, using the MicroPulser Electroporation Apparatus (Bio-Rad). The Sc2 setting (1.5 kV, 25 μF, 200 Ohms) was used with 0.2 cm cuvettes. Transformed cells were resuspended in 1 mℓ 1 M sorbitol and 100 μℓ aliquots were plated on CSM-his plates containing 1 M sorbitol. The correct disruption of the *HHO1* gene was confirmed by PCR of genomic DNA isolated from putative clones (Ausubel *et al.*, 1992). The oligonucleotides primers were designed so that only the genomic DNA, where the *HIS3* gene was correctly incorporated into the *HHO1* open reading frame, would be amplified.

The oligonucleotides used were as follows:

OCC001 5' –GGGGGAATTCTTGATGAAATGCTATTCTGTG- 3', which annealed at the 5' end of *HHO1*.

OCC002: 5' –AATGGCAAGTGATTAACGTC- 3', which annealed within the *HIS3* gene.

The 50 μℓ reaction volume was comprised of 5 μℓ 10 × *Taq* buffer (Roche), 1 U *Taq* DNA polymerase (Roche), 120 μM of each of the deoxyribonucleotide triphosphates, 1.5 mM magnesium chloride (Roche) and 50 pmol of each of the primers. The template DNA (1 ng) was denatured at 94°C for 1 min, followed by 35 cycles of a 1 min denaturing step (94°), 1 min annealing step (50°C) and 45 second extension step (72°C). Finally, partial extension products were allowed to complete by incubating the sample at 72°C for 5 min, after which the sample was kept at 4°C. All subsequent PCR reactions followed the same

program. Successful disruptants were identified by analysing the PCR products on a 1 % (w/v) agarose gel, containing ethidium bromide (10 μg/mℓ) to visualise the bands. Glycerol stocks (15% v/v) were prepared of positive knockout transformants and stored at -70°C.

2.2.4 DNA damage

The ultra-violet radiation sensitivity of a strain was determined by diluting 1mℓ of an overnight culture to a cell density of 2×10^8 cells/mℓ and 2 μℓ of this culture, serially diluted 10-fold, was applied to YPD plates. Plates were irradiated with UV light (0mJ to 5mJ) in a GS Gene Linker UV Chamber (Bio-Rad), before being wrapped in foil. All plates were incubated at 30°C for 2-3 days (Adams *et al*, 1997) before scoring colony growth.

The ionising radiation sensitivity of a strain was determined by diluting an overnight culture to a cell density of 2×10^6. A 200 mℓ quantity of cells was centrifuged (2000 × g, 4°C, 5 min) in a JA 20 rotor (Beckman) and the pellet was resuspended in 6 mℓ sterile 1 × phosphate buffered saline (137mM NaCl, 2.7 mM KCl, 4.3 mM $Na_2HPO_4.7H_2O$, 1.4mM KH_2PO_4). The cells were irradiated with a ^{60}Co point-source irradiator (8.5 Gy/min) with: 0, 300, 600, 900, 1200 and 1500 Gy. A 2 μℓ quantity of each sample, serially diluted 10-fold, was applied to YPD plates. The plates were incubated at 30°C for 2 days (Aboussekhra *et al.*, 1996), before scoring colony growth.

2.2.5 Stress sensitivity

2.2.5.1 Osmotic stress

The sensitivity of a strain to osmotic stress (Weisman and Choder, 2001) was determined by diluting 1 mℓ of an overnight culture to a cell density of 2×10^8 cells/mℓ in water and 2 μℓ of this culture, serially diluted 10-fold, was applied to YPD plates containing 0.5M sodium chloride or 0.6M potassium chloride. The plates were incubated at 30°C for 2-3 days before scoring colony growth.

2.2.5.2 Oxidative stress

The sensitivity of a strain to oxidative stress (Weisman and Choder, 2001) was determined by diluting 1 mℓ of an overnight culture to a cell density of 2×10^8 cells/mℓ and 2 μℓ of this culture, serially diluted 10-fold, was applied to YPD plates containing 5mM hydrogen peroxide. The plates were incubated at 30°C for 2-3 days before scoring colony growth.

2.2.6 Stationary phase expression profiling

2.2.6.1 RNA preparation

RNA was prepared by the "glass bead" method (Ausubel *et al.*, 1992). Aliquots (20 mℓ) were removed from a 500 mℓ FY2 culture in YPD at 24 hour intervals. The cells were pelleted by centrifugation (2000 × g, 4°C, 5min) in a JA 20 rotor (Beckman) and washed with 20 mℓ sterile diethyl pyrocarbonate (DEPC) treated water. The pellet was resuspended in 0.6 mℓ RNA extraction buffer (0.1 M NaCl, 10 mM EDTA, 5 mM Tris-

HCl, pH 7.5) and 0.6 mℓ PCI (50:50:1 of phenol [pH4]: chloroform: isoamyl alcohol). The mixture was incubated at room temperature for 6 minutes and transferred to an eppendorf tube. Acid-washed glass beads, 0.4mm in size (200 μℓ) (Sigma) were added and the samples were vortexed at maximum speed on the Vortex-Genie 2 (Scientific Industries Inc., Bohemia, N.Y., USA). The phases were separated by centrifugation (16 000 × g, 4°C, 20 min). The aqueous layer was transferred to a new eppendorf, and a 0.1× volume of 3 M sodium acetate (pH 5.2) and 2× volumes ice-cold 98 % ethanol were added. To allow precipitation of the RNA, the eppendorfs were transferred to –20°C for one hour and the RNA pelleted by centrifugation (16 000 × g, 4°C, 20 min) and washed with 70% (v/v) ethanol. The RNA pellets were air-dried and resuspended in 50 μℓ DEPC-treated water. The RNA was cleaned using the RNeasy MiniKit (QIAGEN GnbH, Hilden, Germany), according to the manufacturers instructions. RNA was eluted in 60 μℓ nuclease-free water (QIAGEN) and stored at -70°C until use.

2.2.6.2 Northern blot analysis

RNA was electrophoresed on a 0.9% (w/v) formaldehyde-agarose gel, containing 0.05 % (v/v) formaldehyde in a 1× MOPS running buffer (5mM sodium acetate, 20 mM MOPS, 1 mM EDTA, pH7.0). RNA (10 μg) was mixed with 1.5× loading buffer (750 μℓ formamide, 75 μℓ formaldehyde [37 % (v/v), 150 μℓ 10 × MOPS running buffer, 7.5 μℓ ethidium bromide [10 mg/mℓ]), loaded onto the gel, and electrophoresed at 150 V for 6h. After photographing the gel, the RNA was transferred to a nylon membrane (GeneScreen Plus, NEN Life Sciences, Boston, MA, USA), using an overnight capillary transfer

(Ausubel *et a.l*, 1992), with a 5 × SSC (0.75 M NaCl, 75 mM sodium citrate, pH 7.0) buffer. The RNA was cross-linked to the nylon membrane with the GS Gene Linker UV Chamber (Bio-Rad) at 150 mJ.

2.2.6.3 Preparation of DNA probes

DNA probes were produced by PCR. A 770 bp fragment within the *HHO1* coding sequence was amplified and used as a probe for *HHO1* mRNA. The oligonucleotides used were as follows:

OCC003: 5' –CACCCAAGAAATCCACTACCA- 3'

OCC004: 5' –CGTGGAGAGTTTGACCTTCTT- 3'

The 50 μℓ reaction volume comprised 5 μℓ 10 × Taq buffer (Roche), 1 U Taq DNA polymerase (Roche), 120 μM of each of the deoxyribonucleotide triphosphates, 1.5 mM magnesium chloride (Roche) and 50 pmol of each of the primers. The yeast genomic DNA (1 ng) was denatured at 94°C for 1 min, followed by 35 cycles of a 1 min denaturing step (94°C), 1 min annealing step (57°C) and 1 min extension step (72°C). Finally, partial extension products were allowed to complete by incubating the sample at 72°C for 5 min, after which the sample was kept at 4°C.

The 18S rRNA species was used as a loading control, while the gene product of *DNF1* was used as a control for intact mRNA, since actin is not expressed during the stationary phase in yeast (Padilla *et al.*, 1998). *DNF1* was selected by comparing a number of genes that were expressed during the diauxic shift. These genes were identified in the Stanford Saccharomyces Genome database (SGD) available at http://genome-www4.stanford.edu,

using the "Expression Connection" utility (Cherry *et al.*, 1998). An 843 bp fragment within the *DNF1* ORF was amplified and used as a probe for *DNF1* mRNA. The oligonucleotides used were as follows:

OCC005: 5' -ACCGAAGCGTTAGCGGGATTA- 3'

OCC006: 5' -ACAATCCGGAACACCATCTTG- 3'

The PCR reaction conditions were identical to those for *HHO1*, except that an annealing temperature of 47°C was used. PCR products were electrophoresed on a 1 % (w/v) agarose gel containing 10 μg/mℓ ethidium bromide and visualised on a short wavelength UV transilluminator. The band containing the DNA of interest was excised, and the DNA purified using the QIAquick Gel Extraction Kit (QIAGEN).

As stated above, a host of genes were tested for expression through the cell cycle and into the stationary phase. The genes and their corresponding oligonucleotide primer pairs are listed below.

Gene name *BCY1*:

OCC007: 5' –TGGATTTAAGATCGCTTCCC- 3'

OCC008: 5' –CAAAAGACAACAGTAAGAATAAACG –3'

Gene name *ROX3*:

OCC009: 5' – TGGCTTCTAGAGTGGACGAAA- 3'

OCC010: 5' –TCCAGCCTCCTTCTTTTCAT- 3'

Gene name *SNZ1*:

OCC011: 5' –CAGTTAATTATCACGATGACTGGAG- 3'

OCC012: 5' –ATACCTGTTCAAAGAAATCACCACC- 3'

The DNA probes were amplified by PCR, using the same conditions used above, however an annealing temperature of 58°C was used.

2.2.6.4 Labelling and Hybridisation of Probes

DNA was labelled with [α-^{32}P] dCTP (5000 Ci/mmol, Amersham) using the random prime method (Prime-A-Gene Labelling System, Promega) and purified using Nick columns (Pharmacia Biotech, Uppsala, Sweden). Hybridisations were carried out at 65°C in a hybridisation oven (Hybaid Limited, Ashford, Middlesex, UK) and hybridisation tubes rotated at 10 rpm. The nylon membranes were pre-hybridised for 5h in 50 mℓ pre-hybridisation buffer (0.5 % (w/v) non-fat dry milk powder, 0.5 M phosphate buffer [0.5M Na_2HPO_4, 0.5M NaH_2PO_4, pH 6.8], 1mM EDTA, 7 % (w/v) SDS). The buffer was then replaced with pre-heated hybridisation buffer (0.5 M phosphate buffer (pH 6.8), 1 mM EDTA, 7% (w/v) SDS), the radiolabelled probe added, and the hybridisation continued at 65°C for 16h. Following hybridisation, the membranes were washed twice in wash buffer A (5 % (w/v) SDS, 40 mM phosphate buffer (pH 6.8), 1 mM EDTA) at room temperature and once in wash buffer B (1 % (w/v) SDS, 40 mM phosphate buffer (pH 6.8), 1mM EDTA) at 65°C. Washed membranes were exposed to a storage phosphor screen (Kodak) for 16 hours, and visualised using a Personal Molecular Imager FX Phosphorimager (Bio-Rad) and Quantity One software (Bio-Rad). Where membranes were needed to be re-hybridised, hybridised label was stripped by immersion in a boiling solution of 10 mM Tris-Cl (pH 7.9), 1 mM EDTA, 1 %([w/v) SDS for 30 minutes before use. Membranes were stored on blotting paper soaked in TE (pH8) and kept at 4°C when not in use.

2.2.7 Determination of Longevity

Lifespan analyses of W303 and W303-*hho*$^-$ strains were performed by micromanipulation on a Singer MSM System Series 200 (Singer Instrument Co Ltd, Watchet, Somerset, England). Initially, logarithmically growing liquid cell cultures were plated at low density onto YPD plates. The plates were incubated at 30°C for 3 hours. Daughter cells were identified as small buds, and these were separated from mother cells and moved to an unpopulated region of the plate. The lifespan of this cell (now designated the mother cell) was determined by successively moving the larger, mother cell to an identifiable, unpopulated point on the plate, after each division. The plates were incubated at 30°C between manipulations, and stored at 4°C overnight, as described (Kennedy *et al.*, 1995). Lifespan analyses were performed on 10 individual cells for both the WT and *hho1*$^-$ strain. This protocol was adjusted when it was noted that the *hho1*$^-$ cells took longer to recover from the 4°C overnight incubation, and subsequent experiments were done with continual micromanipulation, omitting the 4°C incubation step.

2.2.8 Determination of Cold-sensitive (Cs$^-$) Phenotype

2.2.8.1 Lag phase growth

Single colonies from each strain were picked and inoculated into 10 mℓ YPD medium, and incubated at 30°C with shaking for 16 hours. These cultures were transferred to 4°C for 24 hours, while a duplicate set were left at 30°C without agitation. All samples were diluted to OD_{600} of 0.02 in 50 mℓ YPD and incubated at 30°C with agitation for a 3.5 hour period, with 1 mℓ aliquots being taken at 30 minute intervals. The number of cells in the culture at each time point was determined by measuring the absorbance of aliquots at

600nm. All absorbance readings were taken on a Beckman DU530 Life Science UV/Vis Spectrophotometer. As a control, the lag phase experiment was repeated on a known cold-sensitive mutant strain, YMR 039C (ResGen).

2.2.8.2 Rescue of the phenotype

In order to verify that the lag in cell-cycle progression was caused by the absence of Hho1p as opposed to other background mutations, a centromeric plasmid containing the full-length yeast *HHO1* gene plus the native promoter was constructed and inserted into the *hho1*$^-$ strain.

2.2.8.3 Sub-cloning into pRS416 vector

Plasmid pRS413-yH1 (Patterton *et al.*, 1998) was isolated from *E. coli* strain SURE (Life Sciences) using the Wizard Midiprep System (Promega), according to the manufacturers instructions. The plasmid DNA was eluted in water. A 1.506 kb fragment, containing the *HHO1* ORF and promoter, was excised from the pRS413-yH1 plasmid with *Eco* RI (Promega) and *Xba* I (Promega) restriction enzymes according to the supplier's recommendation. The digested plasmid was electrophoresed on a 1 % (w/v) agarose gel containing 10 µg/mℓ ethidium bromide and visualised by short wavelength UV transillumination. The gel slice containing the *HHO1* fragment was excised, and the DNA purified using the QIAquick Gel Extraction Kit (QIAGEN).

An overnight restriction enzyme digest was performed on pRS416 (Stratagene, La Jolla, CA, USA), using conditions identical to those described above. The digested plasmid was

electrophoresed on a 1 % (w/v) agarose gel at 100 V and visualised by short wavelength UV transillumination. The digested pRS416 plasmid was excised, the DNA purified using the QIAquick Gel Extraction Kit (QIAGEN), and eluted in water.

Plasmid pRS416 (Strategene), digested with *Eco* RI and *Xba* I and purified by gel electrophoresis as described above, was treated with Shrimp Alkaline Phosphatase (Promega). Briefly, 1 U of enzyme per μg of DNA was added to restriction enzyme-digested vector and incubated at 37°C for 15 minutes in 1 × SAP reaction buffer (Promega). The Shrimp Alkaline Phosphatase was heat-inactivated at 65°C for 15 minutes.

The *HHO1* fragment was ligated into the *Eco*RI-*Xba* I digested pRS416 using T4 DNA ligase (Promega). Briefly, 100 ng of *HHO1* fragment and 100ng digested pRS416 was mixed with 1 μℓ 10 × Ligase Buffer (Promega) and 1 μℓ of T7 DNA ligase (Promega, 1 Weiss U/μℓ) in a total volume of 10 μℓ. A background control where the *HHO1* fragment was omitted was also included. All reactions were incubated overnight at 16°C in 1.5 mℓ eppendorf tubes.

The ligation mixture was added to 80 μℓ calcium chloride competent DH5α cells (Stratagene), thawed on ice directly before the transformation procedure. The suspension was mixed gently and incubated on ice for 5 min after which the cells were incubated at 37°C for 10 min. The cells were immediately returned to ice for two min and 910 μℓ of LB medium, pre-warmed to room temperature, was added. Cells were incubated in a

shaking incubator (150 rpm) for 1 hour at 37°C. Aliquots (100 μℓ) were spread on LB plates supplemented with 50 μg/mℓ ampicillin. Plates were grown for a maximum of 14 hrs at 37°C.

Colonies were screened by PCR, using primers OCC003 and OCC004, specific to *HHO1*, described above. Twenty colonies were selected and prepared for colony PCR by placing half a colony (approximately 2 μl of cell paste) in sterile water (50 μl) and incubating it at 95°C for 5 min. A volume of 1μℓ of this sample was used for the PCR reaction. The PCR program was identical to that used in 2.2.6.3 above. PCR products were electrophoresed on a 1 % (w/v) agarose gel agarose gel and visualised by UV transillumination. Positive clones were inoculated into 5 mℓ LB culture medium, supplemented with 50 μg/mℓ ampicillin and grown to an OD_{600} of approximately 0.6. The plasmid was isolated with a Wizard mini-prep DNA purification kit (Promega) as recommended by the supplier, and the presence of the correct insert verified by restriction enzyme analysis. The resultant plasmid was designated pRS416-yH1.

Quantities of 40 μℓ electro-competent W303-*hho1*$^-$ *S. cerevisiae* cells were transformed by electroporation with 100 ng of pRS416-yH1, using the electroporation procedure outlined above. Transformed cells were resuspended in 1 mℓ 1 M sorbitol and 100 μℓ aliquots were plated on CSM-Ura dropout plates containing 1 M sorbitol. The correct insertion of the *HHO1* gene was confirmed by northern blot analysis. This strain was designated W303-*hho1*$^-$ + *HHO1*. Glycerol stocks were prepared and stored at -70°C.

2.2.8.4 Lag Phase growth in presence of "rescue" plasmid

In order to confirm that the insertion of the *HHO1* gene into the W303-*hho1*$^-$ strain rescued the cold-sensitive phenotype, the lag phase was examined in the W303 background strain, its corresponding *hho1*$^-$ strain, as well as W303-*hho1*$^-$ + *HHO1*, using the procedure described in 2.2.8.1 above.

2.3 Microarray Analyses

The level of expression of all genes in *S. cerevisiae* was determined by microarray analysis, using GF 100 nylon membranes containing 6144 yeast ORF DNA spots (ResGen, Invitrogen Corporation, Huntsville, AL, USA). In each set of experiments, one set of membranes was labelled with labelled cDNA extracted from an *hho1*$^-$ strain, while the other set of membranes was labelled with total cDNA from a WT strain.

2.3.1 GeneFilter Microarrays

The Genefilter membranes were prehybridised for 3 hours in a hybridisation roller tube with 5.0 mℓ MicroHyb hybridisation solution (ResGen) and 5.0 µg Poly dA (1 µg/µℓ, ResGen) at 42°C in a hybridisation oven..

The RNA was prepared using the procedure described in 2.2.6.1, and purified using an RNeasy kit (QIAGEN). In a 1.5 mℓ eppendorf, 5 µg total RNA, suspended in 8 µℓ DEPC water (ResGen) was added to 2 µℓ Oligo dT (1 µg/µℓ 10-20 mer mixture, ResGen) for the priming reaction and placed at 70°C for 10 minutes before being placed on ice for two minutes to cool. For the elongation reaction 6.0 µℓ 5× First Strand Buffer (Life

Technologies), 1.0 μℓ DTT (0.1 M, Life Technologies), 1.5 μℓ dNTP mixture without dCTP (20 mM, Pharmacia), 1.5 μℓ [α-^{33}P] dCTP (10 mCi/mℓ, 3000 Ci/mmol, Amersham) was added to the primed RNA, and incubated for 90 minutes at 37°C.

The labelled cDNA/RNA hybrid was purified by passage through a Nick Column (Pharmacia Biotech), using the manufacturers instructions. The purified probe was denatured by placing it in a boiling waterbath for 3 minutes, before adding it to the prehybridised membrane. After hybridising for 16 hours at 42°C, the membranes were washed twice in wash buffer 1 (2 × SSC, 1 % (w/v) SDS) at 50°C and once in wash buffer 2 (1 × SSC, 1 % (w/v) SDS), at 55°C. Washed membranes were exposed to a storage phosphor screen (Kodak) for 16 hours, and visualised using the HP Cyclotron Phosphorimager (Hewlett Packard) and the Quantity One software program (Bio-Rad). Before reprobing, blots were stripped by immersion in a boiling solution of 0.5 % SDS for 1 hour. The Genefilter membranes were analysed using Pathways software (ResGen).

2.3.2 Verification of Microarray data by northern blot analysis

In order to verify the results of the microarray analysis, the expression of the *HHO1* gene was also determined by northern blot analysis. An overnight culture of FY2 cells was transferred to 4°C for 24 hours, diluted to 0.02 and incubated at 30°C for 2 hours with 20 mℓ aliquots being taken at 0; 30 min; 1 hour and 2 hours. Total RNA was extracted using the "glass bead" method described in 2.2.6.1, above. Northern blot analysis was carried out using the protocol outlined in 2.2.6.2, above, again using the *HHO1* probe, prepared by PCR. After stripping, the membranes were re-probed to determine the presence of

core histone mRNAs during the lag phase. Primers specific to Histone H2A and Histone H4 were prepared. A 386 bp fragment within the *HTA1* ORF was amplified and used as a probe for H2A mRNA. The oligonucleotides used were as follows:

OCC013: 5' -TGGTAAAGGTGGTAAAGCTGGT- 3'

OCC014: 5' -ATTCTTGAGAAGCCTTGGTAGCCT- 3'

In the case of the Histone H4 probe, A 307 bp fragment within the *HHF1* ORF was amplified and used as a probe for H4 mRNA. The oligonucleotides used were as follows:

OCC015: 5' –TCCGGTAGAGGTAAAGGTGGTAAA- 3'

OCC016: 5' –AACCACCGAAACCGTATAAGGT- 3'.

The PCR reaction conditions for the amplification of both the H2A and H4 probes were identical to that used for amplifying the *HHO1* probe, though here the annealing temperature used was 57°C.

CHAPTER 3: PURIFICATION AND IDENTIFICATION OF rHho1p

3.1 Introduction

Previous studies have used antibodies to look at the association of chromatin with proteins. In order to elucidate where Hho1p binds in the genome, and to which proteins Hho1p binds, it was necessary to produce rHho1p in large quantities. The protein generated could be used to generate an anti-rHho1p antiserum by injecting the protein into rabbits. The resultant antiserum was immuno-purified as another project in the laboratory. Residual rHho1p was also used for other ongoing projects, however, that is not covered in this study.

Full-length recombinant yeast H1 (rHho1p) was expressed in an *E. coli* strain and purified using a protocol previously described by Patterton and colleagues (Patterton *et al.*, 1998), where using IPTG, Histidine-tagged rHho1p production was induced. The protein was partially purified using Ni^{2+} metal-affinity chromatography and then subjected to CM-Sephadex cation exchange chromatography to further purify the protein. MALDI-TOF analysis was used to verify the identity of rHho1p.

3.2 The expression and purification of rHho1p

The pET-20b (+) bacterial expression system (Novagen) was utilized for the expression of rHho1p in *E. coli*. Expression is driven by an IPTG-inducible T7 promoter, which can be repressed in the presence of T7 lysozyme, expressed from the pLysS plasmid. T7 lysozyme inhibits basal levels of T7 polymerase that is present prior to induction, and

which can lead to counter-selection of plasmids from which toxic peptides are expressed (Baneyx, 1999). IPTG is a synthetic homolog of lactose, which is a natural inducer of expression. IPTG is used for induction of protein expression since it is not hydolysed by β-galactosidase, and therefore the levels of the inducer remain constant throughout the experiment.

The optimal induction time for maximal rHho1p yield was determined by an induction time-course study. An *E. coli* culture (10 mℓ) containing the H1 expression plasmid was induced with IPTG. Aliquots were withdrawn at half hour intervals and the total cellular protein analysed by SDS-PAGE electrophoresis (Figure 3.1). Expression of rHho1p increases as time progresses after the addition of IPTG (lanes 3-8). A 2h induction period produced a maximal amount of recombinant Hho1p in *E. coli*, which is visible in lane 6.

Although the size of rHho1p is 28kDa, the isolated His-tagged protein exhibited anomalous migration on 12% (w/v) SDS-PAGE gels, migrating at a size corresponding to approximately 33kDa (Figure 3.1). This is usual for histones, which are retarded by their charged tails when electrophoresed by SDS-PAGE.

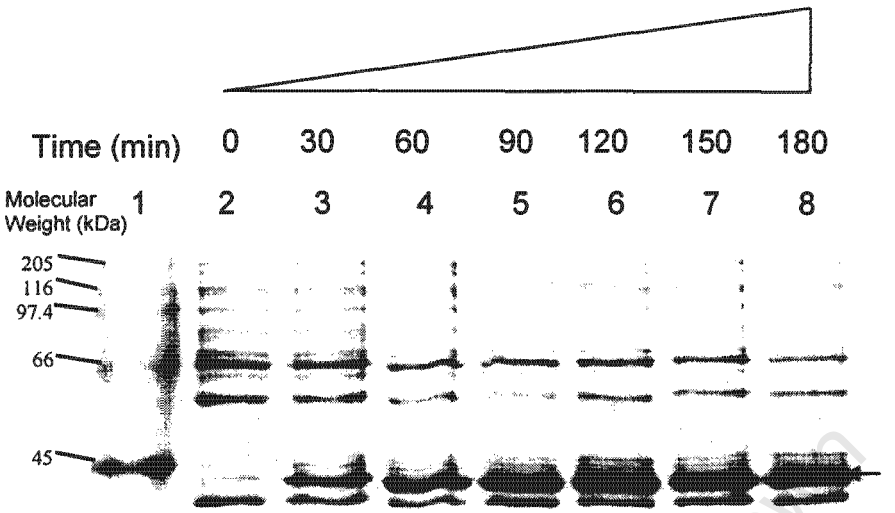

Figure 3.1. Time course induction of rHho1p expression

Aliquots of bacterial culture expressing rHho1p was removed at 30 min intervals following induction (lanes 2 – 8) and electrophoresed on a 12% (w/v) SDS-PAGE gel. A molecular weight marker was run in lane 1, with sizes (kDa) indicated to the left of the figure. An aliquot taken prior to induction was electrophoresed in lane 2. The band that corresponds to rHho1p is indicated with an arrow to the right of the figure.

For a large scale purification, a 1 ℓ culture was grown and after a 2h induction period the cells were harvested and lysed. His-tagged rHho1p was purified by immobilized metal affinity chromatography (IMAC; Sulkowski, 1989), using nickel-agarose resin charged with nickel sulphate (Figure 3.2). The His-tag sequence of the protein binds to Ni^{2+} cations. After unbound proteins are washed away, the target protein is recovered by elution by imidizole, which displaces the His-tag from the Ni^{2+} ions

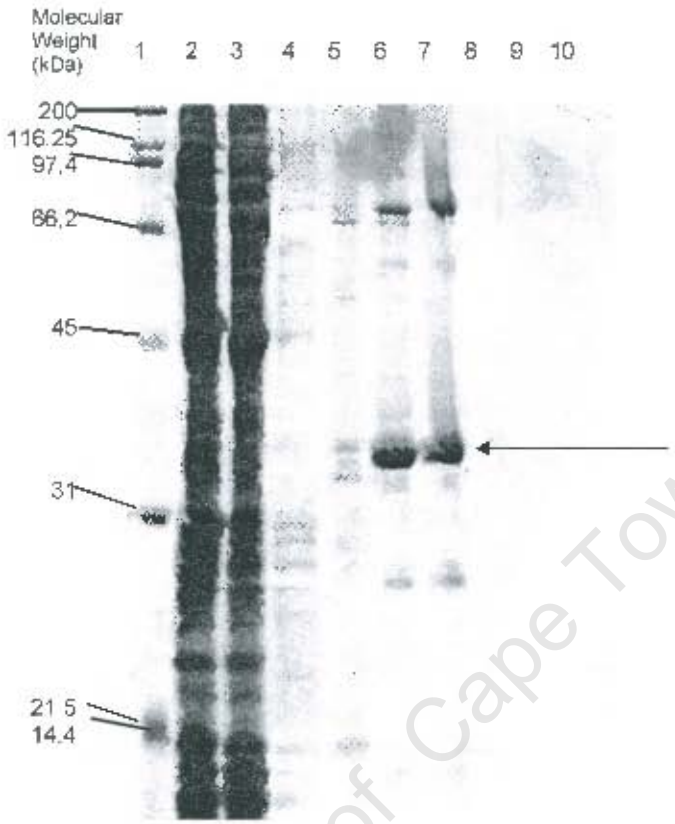

Figure 3.2. Purification of recombinant Hho1p using Ni-agarose chromatography

Aliquots (60 μℓ) of fractions eluted during Ni-chromatography steps were electrophoresed on a 12% (w/v) SDS-PAGE gel and the protein was visualised by Coomassie stain. Lane 1: Broad Range Marker (BIO-RAD); lane 2: crude protein extract; lane 3: binding flow-through; lane 4: binding buffer eluate; lane 5: wash buffer eluate; lane 6 –10: eluted fractions 1 – 5. The arrow on the right of the figure indicates the position of rHho1p.

As shown in Figure 3.2, rHho1p was recovered in elution fraction 1 and 2 (Lane 6 and lane 7), however these fractions contained additional "contaminating proteins", evident by the other bands present. The main contaminants were of sizes 75 and 28 kDa. However, to confirm that the protein was indeed rHho1p, MALDI-TOF mass spectrometry was used to identify the protein.

3.3 In-gel trypsin digest and MALDI-TOF analyses on putative rHho1p

Matrix-assisted laser desorption/ionisation-time of flight (MALDI-TOF) mass spectrometry is a technique where a co-precipitate of an UV-light absorbing matrix and a biomolecule is irradiated with a nanosecond laser pulse. The matrix absorbs most of the laser energy. The ionised biomolecules are accelerated in an electric field and enter a flight tube. During the flight, molecules are separated according to their mass to charge ratio and reach a detector at different times. Therefore, each molecule is able to yield a distinct signal. Each protein has a specific pattern of fragment sizes generated by limited sequence-sensitive trypsin digestion that allows, MALDI-TOF to be used for the identification of proteins.

The proteolytic enzyme, trypsin, catalyses the cleavage of polypeptide chains next to lysine and arginine residues. In-gel trypsin digests and subsequent MALDI-TOF analyses were employed to confirm the identity of the purified protein (Figure 3.3a). Proteins were electrophoresed on a 12% (w/v) SDS-PAGE gel, stained with Coomassie Brilliant Blue and destained, using a methanol-based destain solution. Protein bands of sizes corresponding to rHho1p and carbonic anhydrase (control) were excised from the gel and

treated with trypsin. The eluted trypsin-digested mixtures were analysed by MALDI-TOF. The fragment sizes generated from the trypsin digests for the control protein, carbonic anhydrase, and the putative rHho1p appear in table 1 below.

MS-Fit, a peptide mass fingerprinting tool from the UCSF Mass Spectrometry facility was used to identify the protein. This programme tries to fit the generated mass spectrometry data to a protein sequence in an existing database and thus suggest the identity of the protein of interest. A database search with the digested mass spectrum of rHhop1 identified the trypsin-digested peptide as part of Hho1 from *Saccharomyces cerevisiae*. Hho1p was the only protein identified by this database corresponding to the tryptic fragments analysed by MALDI-TOF. Carbonic anhydrase, isolated from a 12% (w/v) SDS-PAGE gel was used as positive experimental control (Figure 3.3b).

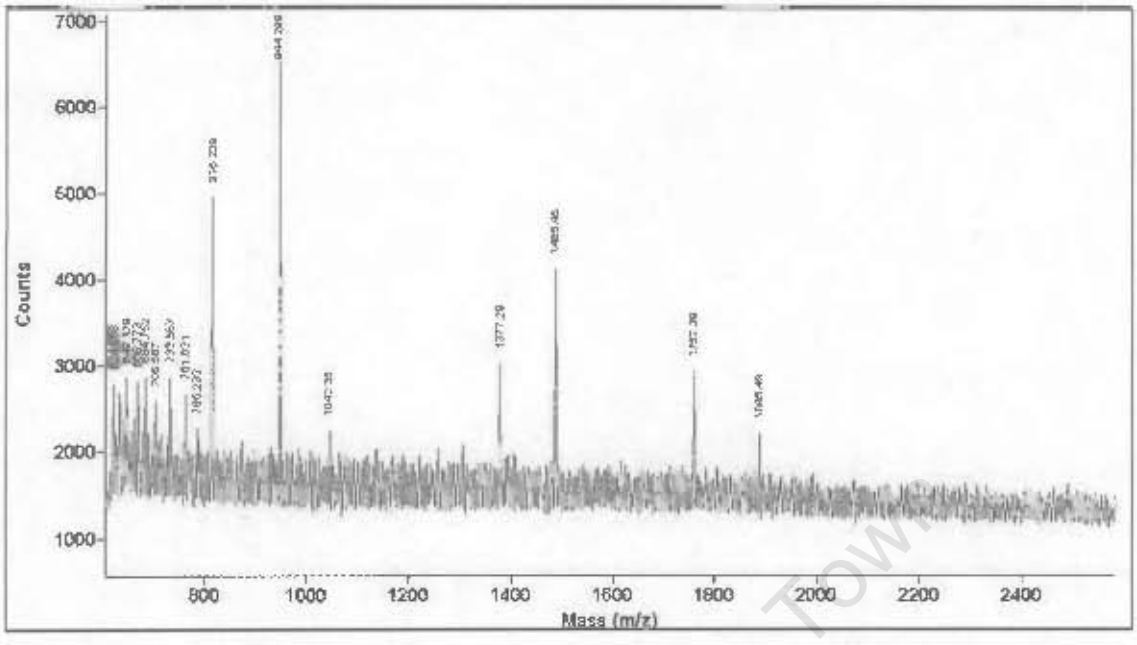

Figure 3.3a MALDI-TOF peak profile for putative rHho1p trypsin digest

The putative rHho1p isolated from an SDS-PAGE gel was subjected to trypsin digestion and MALDI-TOF analysis. The mass spectrum is shown in the figure. The fragment sizes generated from the trypsin digestion were analysed using the MS-Fit program to identify the identity of the protein.

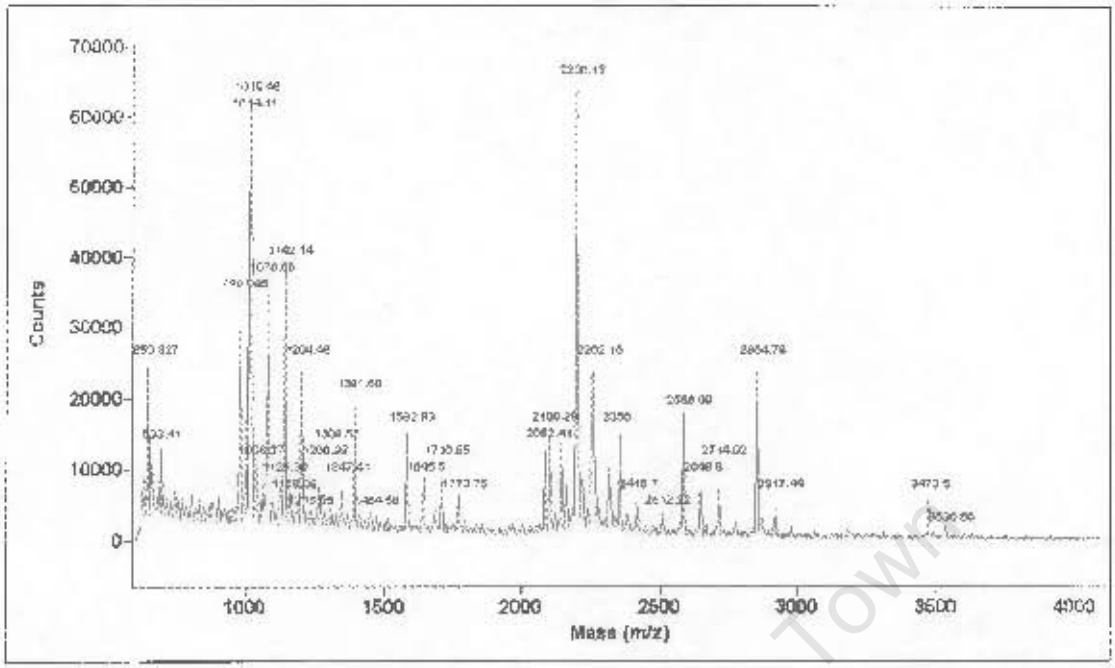

Figure 3.3b MALDI-TOF peak profile for carbonic anhydrase trypsin digest

The carbonic anhydrase isolated from an SDS-PAGE gel was subjected to trypsin digestion and MALDI-TOF analysis. The mass spectrum is shown in the figure. The fragment sizes generated from the trypsin digestion were analysed using the MS-Fit program to identify the identity of the protein.

TRYPSIN DIGEST FRAGMENT SIZES:

Carbonic Anhydrase	Putative rHho1p
1014.11	648.14
1076.66	668.77
1142.14	705.57
1204.48	761.63
1391.69	785.23
1582.83	816.23
2082.41	944.30
2100.29	1042.35
2200.13	1377.29
2586.09	1485.45
2854.79	1751.39
3473.5	1885.48

Table 1: Trypsin digest fragments generated for Carbonic anhydrase and rHho1p.

Fragment sizes generated by MALDI-TOF mass spectrometry after trypsin digests. These were entered into a database to verify the identity of the proteins using the MS-Fit program described.

3.4 CM-Sephadex Purification of rHho1p

Following elution of the rHho1p from the Ni^{2+} column, several contaminating proteins that bound to the Ni^{2+} column were present. In order to purify rHho1p away from these contaminating proteins, an additional chromatographic step was employed. The isolated rHho1p recovered from the metal-chelation chromatography (Figure 3.2 – lane 6 and 7)

was pooled and transferred to a sodium phosphate buffer, using a 10 kDa MWCO ultracentrifugation column, passed over a cation exchange resin, and eluted using a linear NaCl gradient running from 0 M NaCl to 1 M NaCl. However, as is evident in Figure 3.4, the rHho1p was eluted in the flow-through and in the first fraction, contrary to previous determinations (Patterton *et al.*, 1998). This could be attributed to the fact that the gradient-mixer used for producing the linear gradient was inadequate for this purpose.

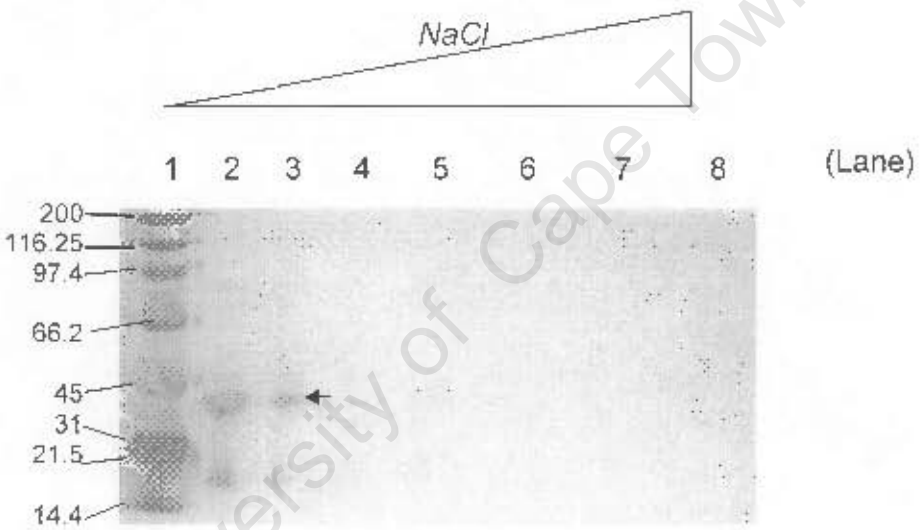

Figure 3.4 Purification of recombinant Hho1p using CM-Sephadex

Cation-exchange chromatography of the Histidine-tagged rHho1p using a CM-Sephadex column. Aliquots (20 $\mu\ell$) of fractions were electrophoresed on a SDS-PAGE gel, and the protein was visualised by Coomassie stain. Lane 1: Broad Range Marker (BIO-RAD); lane 2: flow-through; lanes 3 – 8: eluted fractions 1 – 6. The arrow on the right of the figure indicates the position of rHho1p.

Though the linear gradient does not appear to have worked satisfactorily, the vast majority of contaminating proteins have been removed by the CM-Sephadex column Figure 3.4). Though a contaminating protein ~17 kDa was still present in the fraction, it was decided that Hho1p was present in sufficient quantities for the fractions to be used for anti-serum production.

After CM-Sephadex purification, the band corresponding to Hho1p was analysed by MALDI-TOF. After successful identification as Hho1p, the protein was transferred to 1 × PBS buffer using a 10 kDa MWCO ultracentrifugation column, and stored at 4°C until injection of rabbits for antiserum production.

3.5 Summary

It was necessary to purify rHho1p in large quantities in order to generate an anti-serum against rHho1p. Ni^{2+} metal-affinity chromatography was used to partially purify the protein from an *E.coli* cell culture that had been induced by IPTG for 2 hours. After verifying that the induced protein was Hho1p by MALDI-TOF, rHho1p was purified from contaminating proteins by CM-Sephadex chromatography.

The protein generated was injected into rabbit for antiserum production, however, the immuno-purification of anti-rHho1p antibody was performed as part of another project in the laboratory. The protein and antibody generated will be used as part of chromatin-immuno-precipitation assays in future projects, aimed at further understanding the way Hho1p functions.

CHAPTER 4: PHENOTYPIC CHARACTERISATION

4.1 Introduction

A previous study (Patterton *et al.*, 1998) suggested that the phenotype of an *hho1*⁻ strain would be discovered after such a strain was exposed to various stresses, and the effect on wildtype and *hho1*⁻ cells compared.

Experiments were based on those used in histone H1 deletion studies in other organisms (refer to 1.7). Briefly, *Tetrahymena* becomes more susceptible to DNA damage in the absence of the linker histone (reviewed in Ausio, 2000), which is why this was attempted in yeast. In the tomato plant, cells exposed to water-deficit stress have increased levels of an H1 variant (Scippa *et al.*, 2000), which is why the response to stresses will be tested. Finally, since *Ascobolus* species display a decreased lifespan in the absence of H1, the longevity of *hho1*⁻ will be determined.

4.2 DNA damage

Endogenous and environmental agents frequently damage DNA. Cells have evolved sophisticated systems in response to DNA damage, including DNA repair and cell cycle damage checkpoints (reviewed in Rajpal *et al.*, 2000).

Chromatin conformational changes are evident when H1 is deleted, and the chromatin takes on a more open conformation (Bednar *et al.*, 1998). The nucleosomes are still condensed, but lack the 3D organisation of the 30nm fibre. Chromatin isolated from V-79

Chinese hamster lung fibroblast nuclei by partial digestion with micrococcal nuclease, are more susceptible to radiation damage when H1 is depleted (Heussen *et al.*, 1987), possibly because of the more open chromatin conformation. Pyrimidine dimers are formed by UV irradiation, whereas single and double-strand breaks, DNA-protein crosslinks and base damage are caused by ionising radiation. To assess the role of histone H1 in various DNA damage processes, the response of a H1 deleted strain to UV radiation and γ-radiation was determined.

The ultraviolet sensitivity of *hho1*$^-$ was determined by exposing a serial dilution of wildtype and deletion strain cells to increasing levels of UV radiation ranging from 0 mJ to 5 mJ (Figure 4.1). Little difference is seen between the cell densities of the WT and *hho1*$^-$ strains after being exposed to 1mJ of UV radiation, however at 2mJ, the cell densities of the W303-*hho1*$^-$ strain are less than the W303 WT strain The inverse occurs in the FY2 background strain, where the *hho1*$^-$ strain is less sensitive to UV radiation. This result is more pronounced in the cells irradiated with 4 and 5 mJ of UV radiation.

The results show that the *hho1*$^-$ deletion strain in a W303 background shows increased sensitivity to UV radiation, though the FY2 background strain does not show this sensitivity. The cause for this background effect is uncertain.

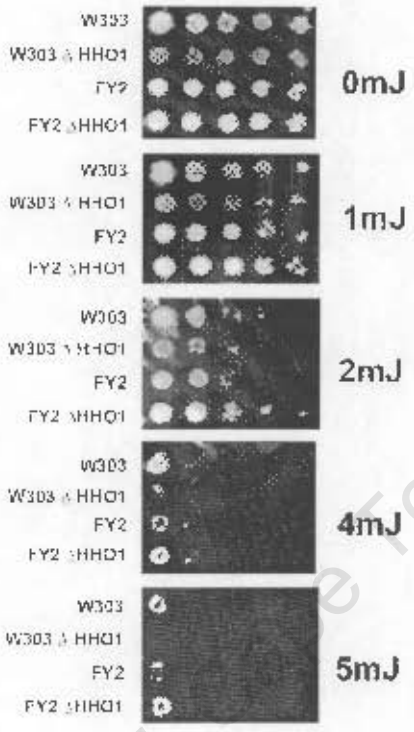

Figure 4.1. The effect of UV sensitivity in the absence of histone H1.

Aliquots of W303 WT, W303 *hho1*, FY2 and FY2 *hho1* were applied as a ten fold dilution series to YPD plates and exposed to UV radiation (254nm) at the radiation doses indicated. The plates were incubated at 30°C for 3 days, and the survival of colonies scored.

The ionising radiation sensitivity of *hho1* was determined by exposing a serial dilution of wildtype and deletion strain cells to increasing levels of ionising radiation ranging from 0 Gy to 1500 Gy (Figure 4.2).

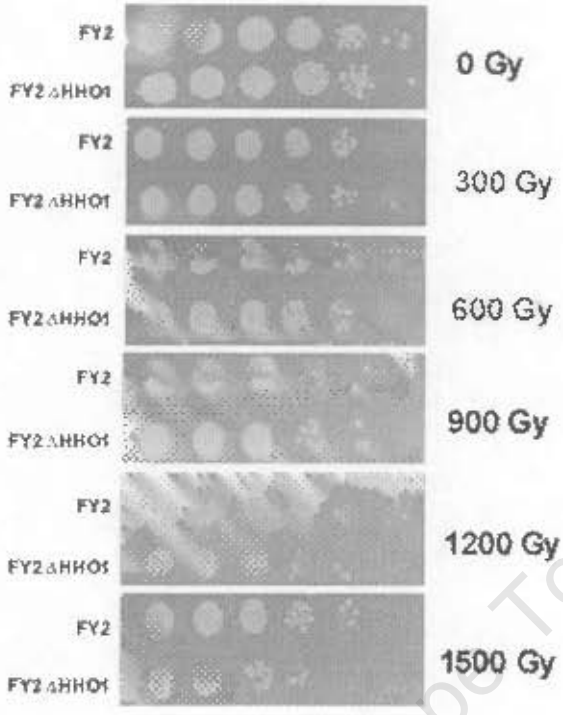

Figure 4.2 The effect of ionising radiation in the absence of histone H1.

Aliquots of FY2 and FY2 *hho1*$^-$ (2μℓ) were exposed to a Co^{60} Point-Source Irradiator at the radiation doses indicated, and applied as a ten-fold dilution series to YPD plates. The plates were incubated at 30°C for 2 days, and the survival of colonies scored.

Little difference is seen between the cell densities of the WT and *hho1*$^-$ strains after being exposed to 300-900 Gy of γ-radiation, however at 1200 Gy, the cell densities of the *hho1*$^-$ strain are less than the WT strain. This result is more pronounced in the cells irradiated with 1500 Gy of γ-radiation. This experiment was only performed in FY2 cells.

The results show that the *hho1*⁻ strain shows a greater sensitivity to ionising radiation compared to the FY2 wildtype strain. This might imply a role for DNA repair for Hho1p.

4.3 Stress sensitivity

Different types of environmental and physiological stress conditions constantly challenge all organisms. To cope with the effects of stress, cells have developed rapid molecular responses to repair the damage and protect against further exposure to the same and other forms of stress (reviewed by Estruch, 2000). Intriguingly, histone H1 was previously shown to be involved in a stress response. The levels of histone H1 were shown to rise in the leaves of tomato leaves exposed to water deficit stress (Scippa *et al.*, 2000), and it was therefore decided to determine whether the *hho1*⁻ strain was more susceptible to stress conditions (Figure 4.3).

The control of water content is essential for all types of cells. When yeast is exposed to a hyperosmotic shock a loss of cytoplasmic water occurs and several mechanisms are initiated to counteract cell dehydration and protect the cellular structures. Little difference is seen in the cell densities of *hho1*⁻ and WT cells when exposed to osmotic stress inducers like NaCl and KCl (Figure 4.3), when compared to the control plate.

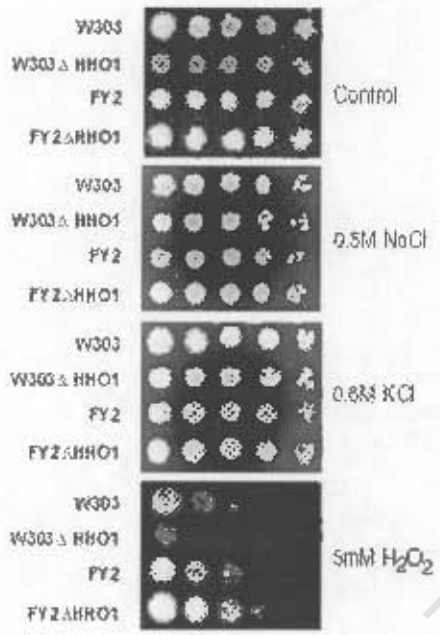

Figure 4.3. The effect of osmotic and oxidative stress in the absence of histone H1.

Aliquots of W303 WT, W303 *hho1*, FY2 and FY2 *hho1* were applied as a ten fold dilution series to YPD plates containing NaCl or KCl in the case of osmotic stress and H_2O_2 in the case of oxidative stress. The plates were incubated at 30°C for 3 days, and the survival of colonies scored.

Aerobically growing yeast have to handle the generation of reactive oxygen species such as hydrogen peroxide or hydroxyl radicals. These oxygen species are generated by normal metabolic processes as well as exposure to pro-oxidants such as H_2O_2. This is evident in Figure 4.3. The cell densities of the FY2 WT strain are less than its corresponding *hho1*⁻ strain when plated on H_2O_2 plates. The converse is true for W303 where, very little cell growth is seen in the deletion strain. The sensitivity of the H1 deletion strain to oxidative stress seems to be strain specific since only the W303 strain exhibited this phenomenon.

4.4 Stationary phase expression profiling

The chromatin of stationary phase yeast cells is in a tighter conformation than in logarithmically growing cells (Lohr and Ide, 1979). Since, histone H1 is involved in the higher order compaction of chromatin into the 30 nm fibre, it may play a role during this stationary phase compaction. It was therefore decided to examine the stationary phase expression profile of the *HHO1* gene in yeast.

Before this could be done, it was necessary to find a gene that was constitutively expressed through logarithmic growth and into the stationary phase, since actin, which is commonly used as an internal control for logarithmically growing cells, is not expressed during the stationary phase (Padilla *et al.*, 1998). Genes were chosen from those showing constitutive expression up to the diauxic shift. However, as is evident in Figure 4.4, only *DNF1*, a potential aminophospholipid translocase, was expressed constitutively during logarithmic and stationary phase growth.

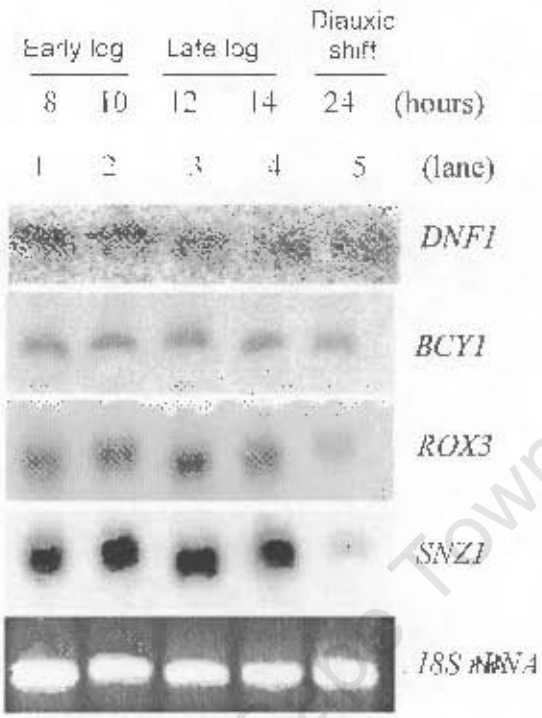

Figure 4.4. The expression of early stationary phase genes during log phase and early stationary phase.

In order to find a control gene that was constitutively expressed throughout the cell cycle and into the stationary phase, various diauxic shift and early stationary phase genes were tested. The 18S rRNA band was used as a loading control. Hours 8 – 10 correspond to early log phase, 12 – 14 correspond to late log phase, while 24 h corresponds to the diauxic shift.

BCY1, *ROX3* and *SNZ1* were expressed constitutively in early log and late log phase (lanes 1-4, Figure 4.4). However, the mRNA expression of these genes decreased markedly when the cells reached the diauxic shift (lane 5). The only gene that showed constitutive expression throughout the cell cycle was *DNF1*, which displayed roughly equal levels of mRNA expression in the early log and late log phases of the cell cycle. The mRNA expression remained constant for *DNF1* as the cell entered into the diauxic

shift (lane 5) and the gene was therefore used as an internal control for the presence of mRNA in future experiments.

Yeast cultures were grown for 5 days with samples removed for RNA extraction each day, over a 5 day period, to determine whether *HHO1* was expressed during the stationary phase. Using northern blot analysis it was found that *HHO1* was expressed at constant levels during the stationary phase, from 1 day to 5 days (Figure 4.5). *DNF1* which was used as a control for intact mRNA was also expressed at constant levels during the stationary phase over the 5 day period.

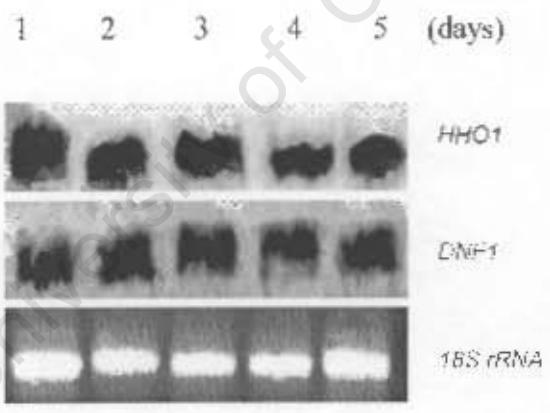

Figure 4.5. The stationary phase expression of histone H1.

RNA was extracted at 24 hour intervals over 5 days from W303 yeast cultures and probed for the presence of *HHO1* mRNA. *DNF1* was used as a constitutive expression control, while the 18S rRNA band was used as a loading control.

4.5 Determination of Lifespan

The absence of histone H1 in *Ascobolus* causes a decrease lifespan in the organism, with growth ceasing within 6 – 13 days (Barra *et al.*, 2000). The lifespan analysis of a W303 and W303 *hho1*⁻ strain was performed using a micromanipulator and the number of cell division events was determined. The lifespan of a mother cell was determined by counting the number of daughter cells produced before senescence was reached.

As is evident in Table 2, the absence of histone H1 does not affect the lifespan of the yeast cell, with both the wildtype and *hho1*⁻ strain going through an average of 26 cell divisions.

Table 2. The influence of histone H1 on the longevity of yeast.

Strain	Cell divisions
W303	26 ± 3 (n = 10)
W303 HHO1Δ	26 ± 2 (n = 10)

The longevity of W303 and W303 *hho1*⁻ strains were determined by quantitating the number of cell divisions that a single yeast mother cell completed. It was noted that the mutant strain displayed a lag in growth after overnight 4°C incubation. Whereas the WT strain was able to produce a bud within 3 hours after the overnight (4°C) incubation, the *hho1*⁻ took up to 6 hours to produce a bud. The possibility of the mutant strain possessing a cold-sensitive phenotype was therefore investigated.

4.6 Determination of Cold-sensitive (Cs^-) Phenotype

The lag phases of the FY2 and W303 background strains and their corresponding H1 deletion strains were examined by reading their absorbances at 30 minute intervals over a period of 3.5 hours. A known cold-sensitive mutant, *YMR039C*, was used as a control (Figure 4.6).

The results show that the mutant strains show decreased growth over the lag phase. Both W303-*hho1*$^-$ and FY2-*hho1*$^-$ showed slowed growth during the lag phase when compared to their WT counterparts. So as to verify that the lag in cell-cycle progression was caused by the absence of Hho1p as opposed to other background effects, a centromeric plasmid containing the full-length yeast *HHO1* gene plus promoter area was constructed and inserted into the *hho1*$^-$ strain.

In order to confirm that the insertion of the *HHO1* gene into the W303-*hho1*$^-$ strain rescued the cold-sensitive phenotype, the lag phase was examined in the W303 background strain, its corresponding *hho1*$^-$ strain and W303- *hho1*$^-$ + *HHO1* (Figure 4.7). The deletion strain with the inserted *HHO1* plasmid has comparable growth to the WT strain. The *hho1*$^-$ strain has slower growth during the lag phase when compared to the "rescued" and WT strains.

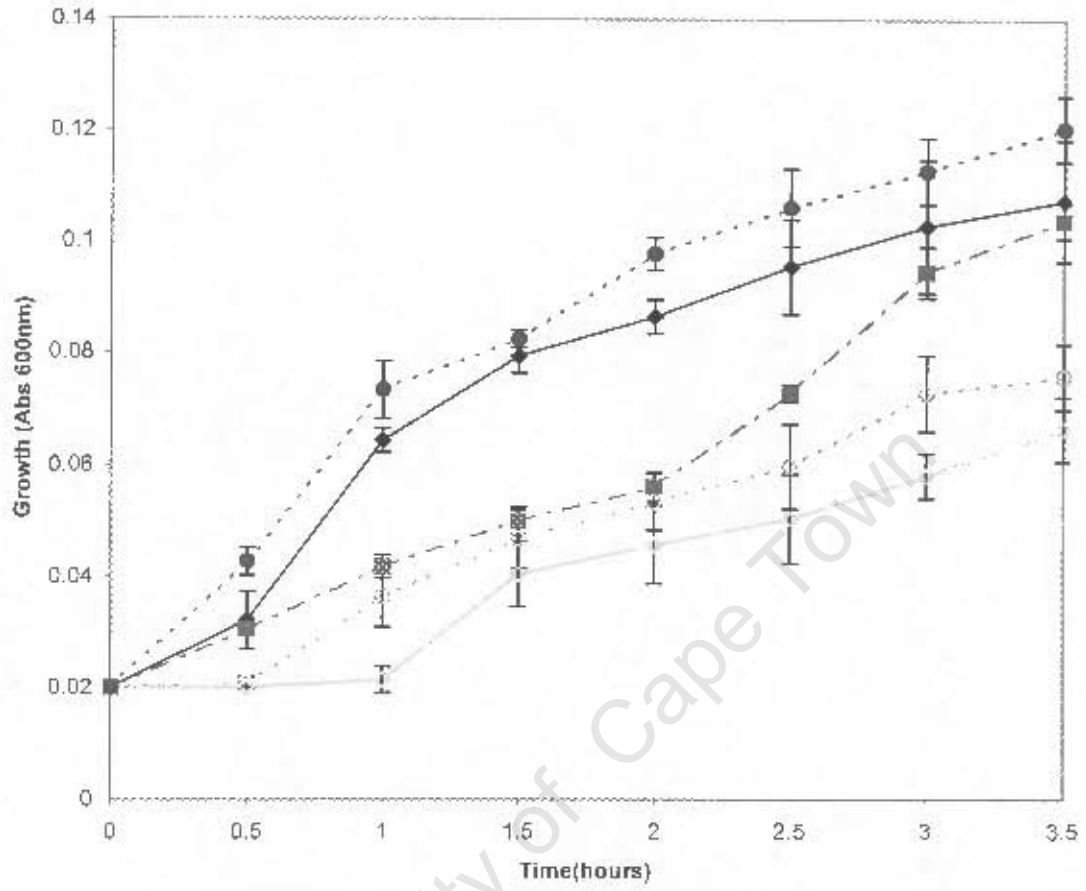

Figure 4.6. The growth of WT and *hho1*⁻ strains following exposure to 4°C.

Growth (OD_{600}) was plotted versus time (minutes). W303 (closed circles), W303 *hho1* (open circles), FY2 (closed diamonds) and FY2 *hho1*⁻ (open diamonds) were grown to stationary phase and incubated at 4°C for 24 hours. Cultures were diluted to OD_{600} of 0.02 and incubated at 30°C for up to 3.5 hours. A known cold-sensitive strain, *YMR039C*, was used as a control (indicated by the closed squares).

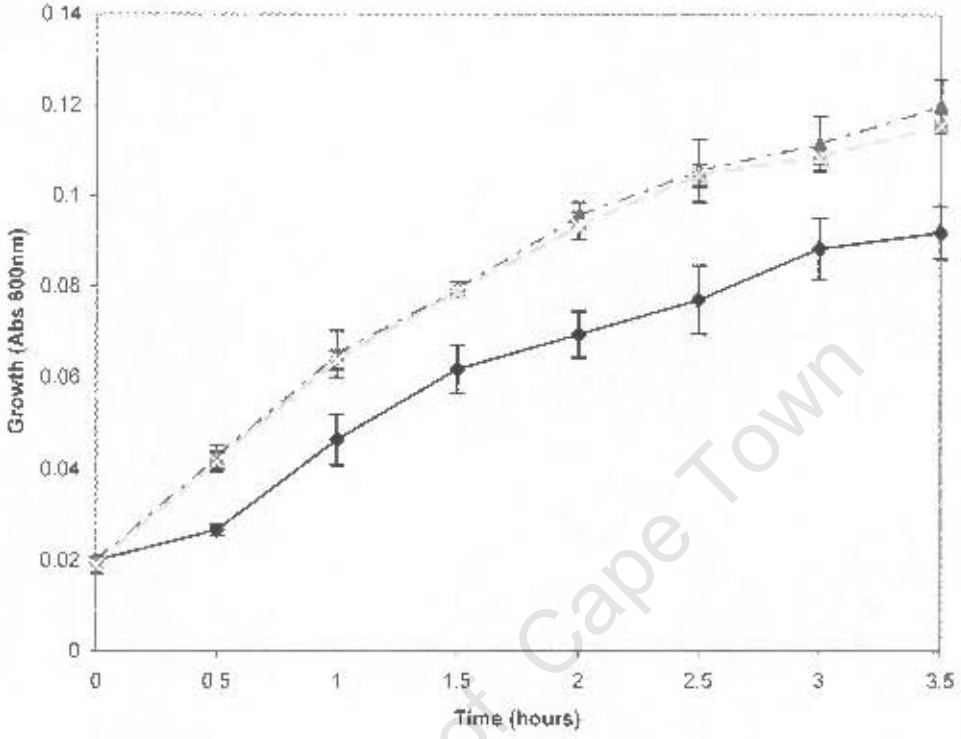

Figure 4.7. The rescue of the cold-sensitive phenotype.

Growth (OD_{600}) was plotted versus time (minutes). W303 (closed squares), W303 *hho1* (closed diamonds), W303 *hho1* + *HHO1* (closed triangles) were grown to stationary phase and incubated at 4°C for 24 hours. Cultures were diluted to OD_{600} of 0.02 and incubated at 30°C for up to 3.5 hours.

To verify that the *HHO1* mRNA was present in the *hho1*⁻ strain, northern blot analysis was used (Figure 4.8). In this experiment the expression of *HHO1* was compared in two *hho1*⁻ strains, a wildtype strain, and an *hho1*⁻ containing a rescue plasmid.

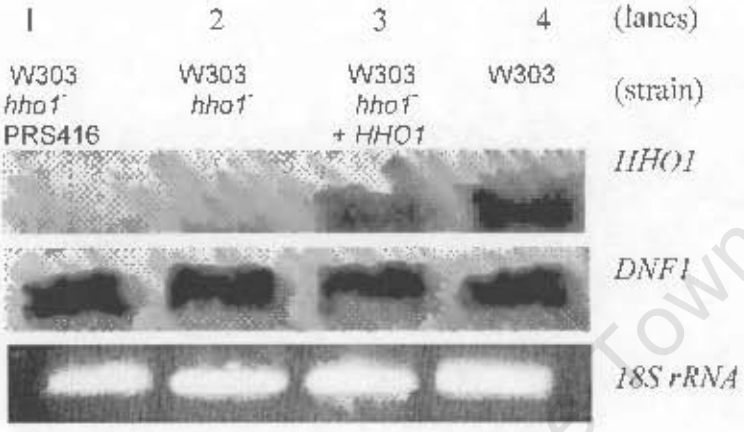

Figure 4.8. Northern blot confirming the expression of HHO1 in W303 *hho1*⁻ after insertion of a rescue plasmid.

W303 *hho1*⁻ was transformed with a centromeric plasmid containing the *HHO1* gene and its promoter regions. RNA was extracted from the resultant strain designated W303 *hho1*⁻+ *HHO1* to confirm that *HHO1* was expressed. Lane 1: W303 *hho1*⁻+ plasmid (no *HHO1*); Lane 2: W303 *hho1* (knockout strain); Lane 3: W303 *hho1*⁻+ *HHO1* (knockout +H1 gene); Lane 4: W303 (WT).

In the W303 *hho1*⁻ strain (lane 1), no *HHO1* mRNA transcript occurs because no functional *HHO1* gene occurs in this strain, since an empty plasmid vector, without the *HHO1* gene was transformed into this strain. No mRNA transcript is seen in lane 2 either, since this is the knockout strain, which does not possess a functional *HHO1* gene. It is evident that the wildtype strain (lane 4) and the *HHO1* deletion strain containing the H1 insert (lane 3), possess *HHO1* mRNA, while the knockout strains do not. *DNF1* was used as a control for intact mRNA, while 18S rRNA was used as a loading control. This result confirms that a functional *HHO1* gene occurs in the W303 *hho1*⁻ + *HHO1* strain.

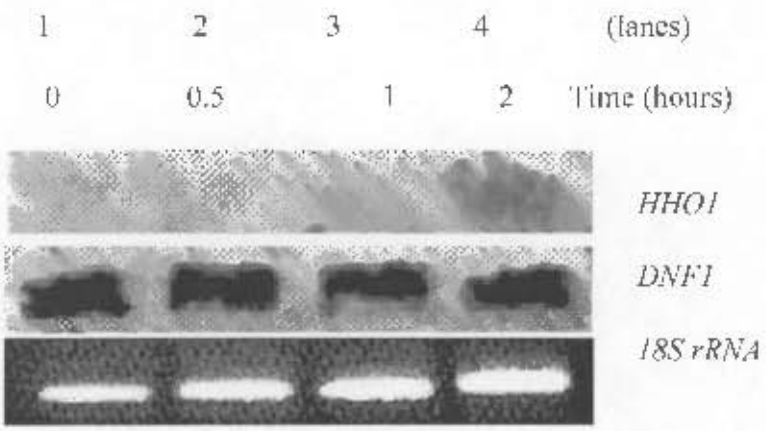

Figure 4.9. Northern blot displaying the expression pattern of *HHO1* during the lag phase.

RNA was extracted at intervals during the lag phase following a 24 hour 4°C incubation and probed for the presence of *HHO1* mRNA. The *DNF1* was used as a constitutive expression control, while the 18S rRNA band was used as a loading control. 0h refers to RNA at the start of lag phase after the 4°C incubation; 0.5h – refers to 0.5 h after the start of lag phase. Samples were also taken 1h and 2h after the start of lag phase.

It was necessary to test whether *HHO1* mRNA was present during the lag phase, since this was when the phenotype was visible. RNA was extracted from cell aliquots removed at 30 minute intervals during the lag phase. The cells had been incubated at 4°C overnight, before being diluted to a cell density of 0.02, and incubated at 30°C to allow growth. Northern blot analysis (Figure 4.9) was used to determine the presence of *HHO1* mRNA, at intervals during the lag phase. No *HHO1* mRNA transcript was present at 0 to 1 hour of growth (lanes 1-3), though *HHO1* mRNA was detected at 2 hours (lane 4). *DNF1*, the control for intact mRNA, was expressed constantly throughout the 2 hour period. Therefore Hho1p might be synthesised earlier during the lag phase, persisting through cold shock, even though the expression of *HHO1* is switched off during cold shock.

4.7 Summary

The phenotypic characterisation examined the response of *hho1*$^-$ strains to various stresses. Though the *HHO1* strain is not affected by osmotic or oxidative stress, and does not show a decreased lifespan, it does display sensitivity to DNA damage, which may implicate Hho1p in protecting chromatin from DNA damage. Furthermore, the *hho1*$^-$ strain displays a cold-sensitive phenotype. Though this phenotype presents itself during the lag phase, no *HHO1* mRNA is present in WT cells during the lag phase. In order to explain the cold-sensitive phenotype, the gene expression levels of all yeast genes needs to be investigated during the lag phase. Furthermore, the levels of Hho1p during the lag phase should also be determined.

CHAPTER 5: MICROARRAY

5.1 Introduction

Following the complete sequencing of the yeast genome in 1996 (Goffeau *et al.*, 1996), and the development of DNA microarrays (DeRisi *et al.*, 1997; Wodicka *et al.*, 1997), it became possible to investigate the gene expression profile of the complete genome in response to environmental conditions or genetic modifications. Numerous microarray studies have been performed on yeast. Spellman and colleagues (Spellman *et al.*, 1998) examined the expression of yeast genes at different points during the cell cycle. Further studies have examined gene expression in meiosis (Cho et al., 1998), in response to heat shock treatment (Roth *et al.*, 1998) and in response to mutations in transcription factors (Holstege *et al.*, 1998). The results and data of numerous such studies can be accessed at dedicated sites on the internet, like the yeast microarray global viewer at http://transcriptome.ens.fr/ymgv/ (Marc *et al.*, 2001).

The cell cycle microarray study (Spellman *et al.*, 1998) showed that the *HHO1* gene reached a peak in expression during the M-phase of the cell cycle. Two studies investigating the response of the yeast transcriptome to the absence of Hho1p were recently published (Hellauer *et al.*, 2001; Freidkin and Katcoff, 2001). Both studies reported a modest decrease (<2 ×) in the general transcription level on a genome-wide scale. These results therefore suggested that it was unlikely that Hho1p acted as a general transcriptional repressor. However, both these studies used probes prepared from cells under conditions where no phenotype for the *hho1*$^-$ strain was visible. It is expected that under these conditions, the absence of Hho1p will have minimal effect on the transcriptome.

5.2 Explanation for the cold-sensitive phenotype

In this study we have identified a clear phenotype, where a yeast strain lacking Hho1p, takes up to 3 times longer to produce a bud following exposure to 4°C. This temporary pause was also visible as a lag phase of approximately 2h before resumption of growth, after exposure of a stationary phase culture to 4°C. Since we have shown that this lag phase was rescued by Hho1p, it is clear that the cold-sensitive phenotype is due to the absence of Hho1p.

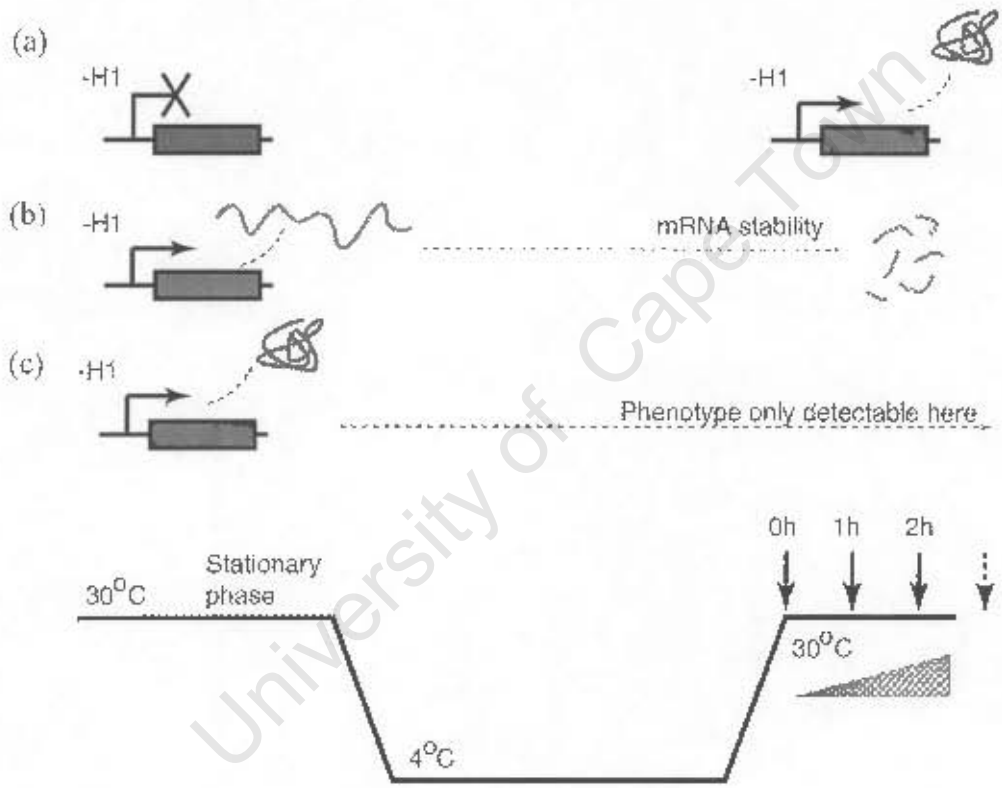

Figure 5.1 What will the microarray tell me?

a) Gene is inappropriately repressed or activated in the absence of Hho1p following the nutrient limited stationary phase and cold-treatment; b) An effect on the mRNA half-lives of transcripts, detected by the microarray during the lag phase; c) Genes may be inappropriately regulated prior to cold-treatment in the absence of Hho1p, but where the gene product is directly involved in establishing the cold-sensitive phenotype.

The link between the phenotype and Hho1p might be co-incidental. For instance, a gene identified in one of the previous microarray studies of the *hho1*⁻ strain may be slightly repressed, which resulted in a modified cell wall, for instance, which is then detectable as a cold-sensitive trait. Alternatively, the absence of Hho1p may cause a direct effect on gene expression during the cold treatment, resulting in the detected phenotype. The simplest model is where a gene is inappropriately repressed or activated in the absence of Hho1p following the nutrient limited stationary phase and cold-treatment (Figure 5.1) Alternatively, a gene may be inappropriately regulated prior to cold-treatment in the absence of Hho1p, where the gene product is directly involved in establishing the cold-sensitive phenotype, by elevated levels of stress response factors, for instance. In this case, the causative gene expression profile will not be detected under the phenotypic conditions, but during stationary phase. It is also possible that the cold-treatment may have an effect on the mRNA half-lives of transcripts, and that the expression profile detected under phenotypic conditions may reflect this effect in addition to a direct transcriptional regulating effect. It was therefore decided to perform the microarray analysis of the transcriptome at different times to address the different possible transcriptional models that can result in the observed cold-sensitive phenotype.

The difference in gene expression between WT and *hho1*⁻ cells was determined using Genefilters yeast microarrays, containing the DNA of 6144 ORFs in the yeast genome. Briefly, total RNA was reverse transcribed and simultaneously radioactively labelled by incorporation of [α-^{33}P] dCTP. The labelled probe was purified and used in a hybridisation experiment, and the level of mRNA corresponding to each ORF quantitated with a phosphorimager and microarray analysis software.

5.3 Lag phase microarray – the start of lag phase (0h)

Stationary phase yeast cells are quick to respond to their environment when suitable nutritional conditions return, and genes required to metabolise these nutrients are quickly activated (Padilla *et al.*, 1990; reviewed by Werner –Washburne *et al.*, 1993). The 0h lag phase time point therefore contains cells that have been returned from starvation conditions.

Microarray data that shows a less than 2 × difference in expression for genes have been shown to have a high error rate, and we therefore decided to analyse only those genes showing a 3 × difference in expression. A total of 118 genes were found to show an up – or down regulation of 3 × or more. In order to see whether the absence of Hho1p affected a specific class or classes of genes, genes that displayed a regulatory dependence on Hho1p were grouped according to the Eurofan functional category (Mewes *et al.*, 1997), shown in Table 3.

European Functional Analysis Projects (Eurofan)	
Functional Classification	
1.	Metabolism (1065 ORFs)
2.	Energy (252 ORFs)
3.	Cell Growth, Cell Division And DNA Synthesis (838 ORFs)
4.	Transcription (793 ORFs)
5.	Protein Synthesis (359 ORFs)
6.	Protein Destination (588 ORFs)
7.	Transport Facilitation (310 ORFs)
8.	Cellular Transport And Transport mechanisms (497 ORFs)
9.	Cellular Biogenesis (206 ORFs)
10.	Cellular Communication/Signal Transduction (133 ORFs)
11.	Cell Rescue, Defense, Cell Death And Ageing (364 ORFs)
12.	Ionic Homeostasis (124 ORFs)
13.	Cellular Organization (2259 ORFs)
14.	Transposable Elements, Viral And Plasmid Proteins (116 ORFs)
15.	Classification Not Yet Clear-Cut (149 ORFs)
16.	Unclassified Proteins (2425 ORFs)

Table 3. Eurofan Functional Classification.

Categories are listed with the number of ORFs in each category indicated in brackets.

The grouping of the responsive genes is shown in Figure 5.2. Since each functional class contains different numbers of members, the number of Hho1p responsive genes were normalised to the number of members in the class, the result of which is shown in Figure 5.3.

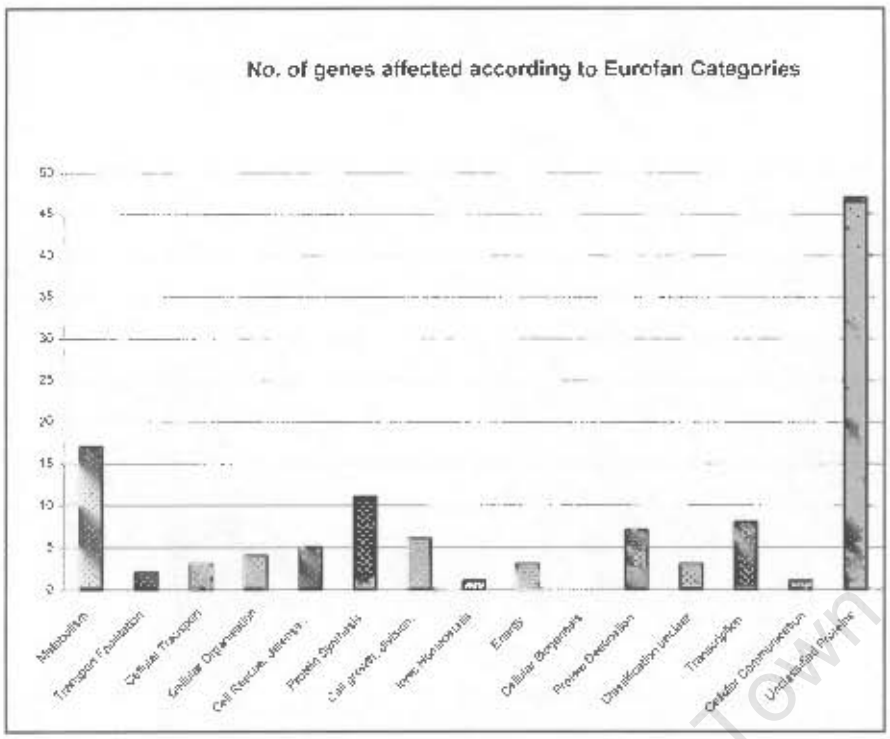

Figure 5.2 The number of genes affected according to Eurofan functional groups (0h).

The bar-graph shows the number of genes at the beginning of lag phase (0h) in each functional category affected by the deletion of *HH01*, after a 4°C incubation. The number of genes is plotted on the y-axis.

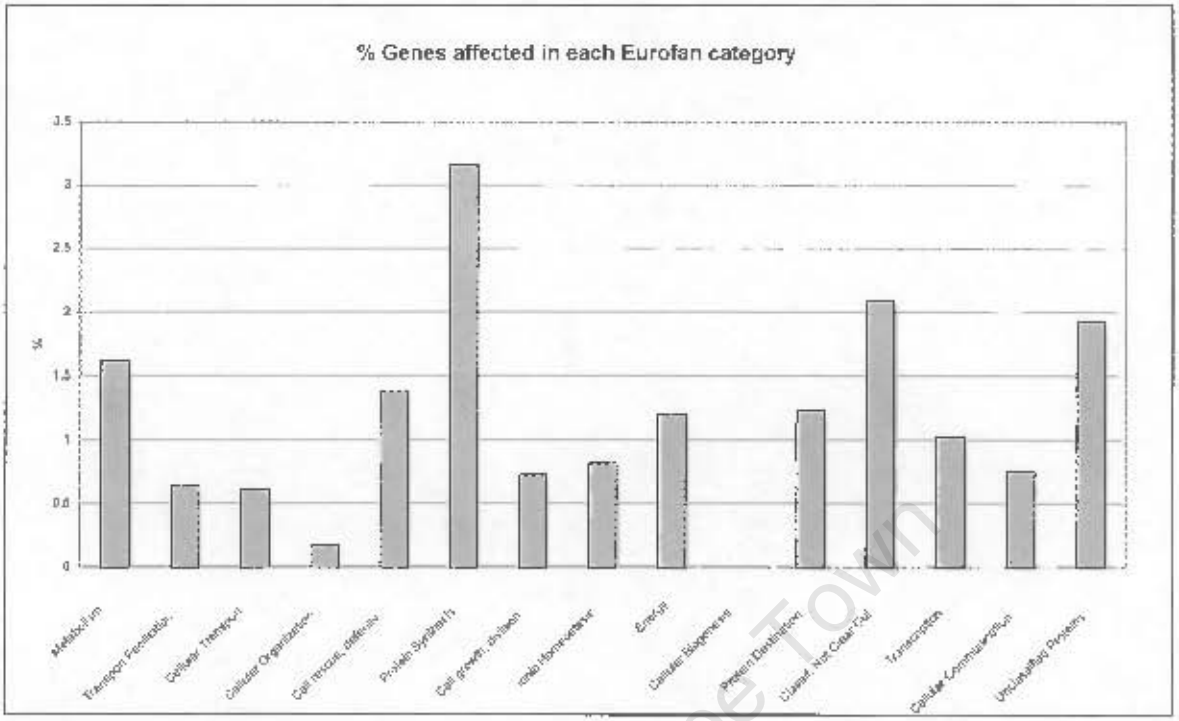

Figure 5.3 The percentage of genes affected according to Eurofan functional categories. The bar-graph shows the % of genes at the beginning of lag phase (0h) in each functional category, affected by the deletion of *HHO1*, after a 4°C incubation. The % of genes is plotted on the y-axis.

These data show that genes in a broad spectrum of functional classes are affected when Hho1p is absent. Furthermore, it does not appear that a single functional class is preferentially affected by the absence of Hho1p.

To investigate the possibility that the genes that respond to Hho1p do so not because of a functional classification, but due to localised Hho1p-dependent chromatin structures, the location of the responsive genes were noted on the chromosomes (Saccharomyces Genome Database). Interestingly, on chromosome IV and VII, the

genes affected were shown to be in the same area of the chromosome (Figure 5.4). The other chromosomes did not exhibit clustered regions of genes affected by the absence of Hho1p.

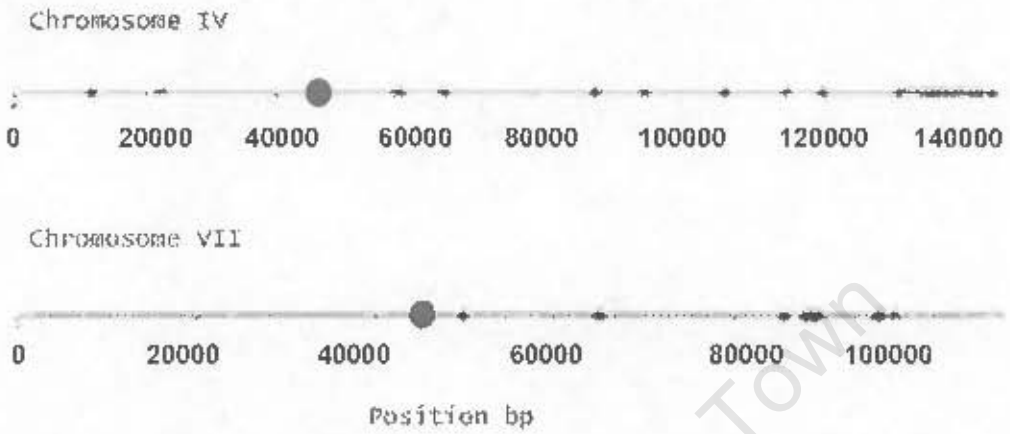

Figure 5.4 Clusters of genes affected by the absence of *HHO1* at the beginning of lag phase. Genes (ORFs) are indicated by the coloured diamonds. Centromeres are indicated by the maroon dots. Chromosome length (bp) is indicated.

It is important to note that while these genes occur in physical clusters on the chromosomes, they are situated on different areas of the GeneFilters yeast microarrays. Also, genes in the identified clusters displayed both activation and repression in the absence of Hho1p, although the majority of genes were up regulated in the WT cell. Interestingly, the genes present in the large cluster on chromosome IV at the 0h lag time point, are all upregulated. This is evident in Figure 5.5, which shows this clustered region in greater detail.

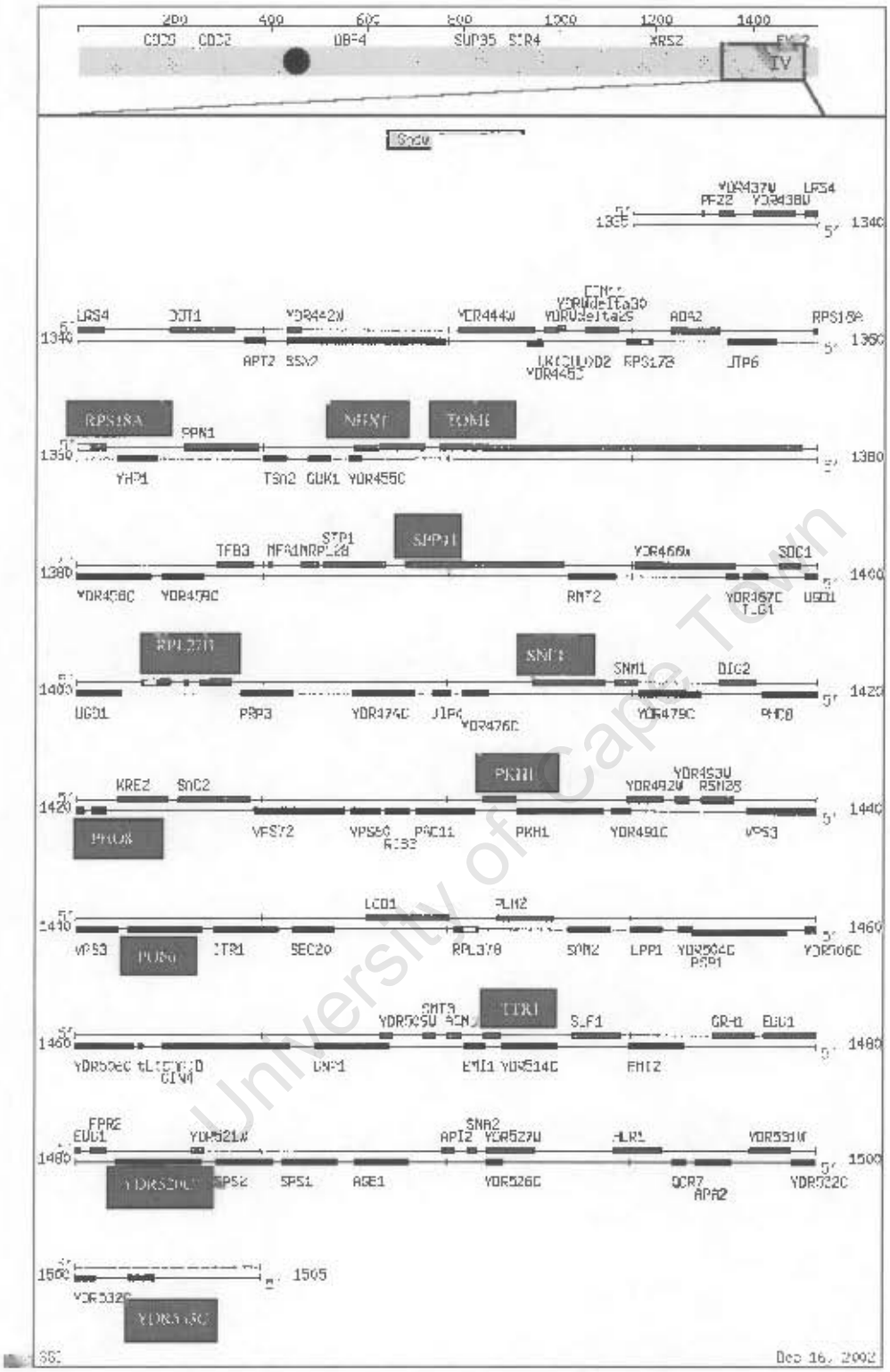

Figure 5.5 Large clustered region on chromosome IV at the 0h – lag time point.

Genes affected by the absence of *HHO1* are indicated by the red rectangles.

The genes in this region are not confined to any functional group, and interestingly, none of them are down-regulated.

5.4 Lag phase microarray – 1h time point

RNA was extracted one hour after the start of lag phase. The differences in gene expression for the 1h time point were determined using the same procedure used above. However, in this case, total RNA was extracted from cells one hour into the lag phase. This was performed to investigate the transcription profile in the *hho1*⁻ at a time when it was likely to more closely resemble that of the WT strain.

A total of 216 genes were found to be affected by the absence of Hho1p at this stage of growth. These genes were classified as described above. Figure 5.6 shows the number of genes in each functional class and the percentage of genes in each functional class affected by the absence of the *HHO1* gene is shown in Figure 5.7. Again the genes affected are not restricted to any one class of genes.

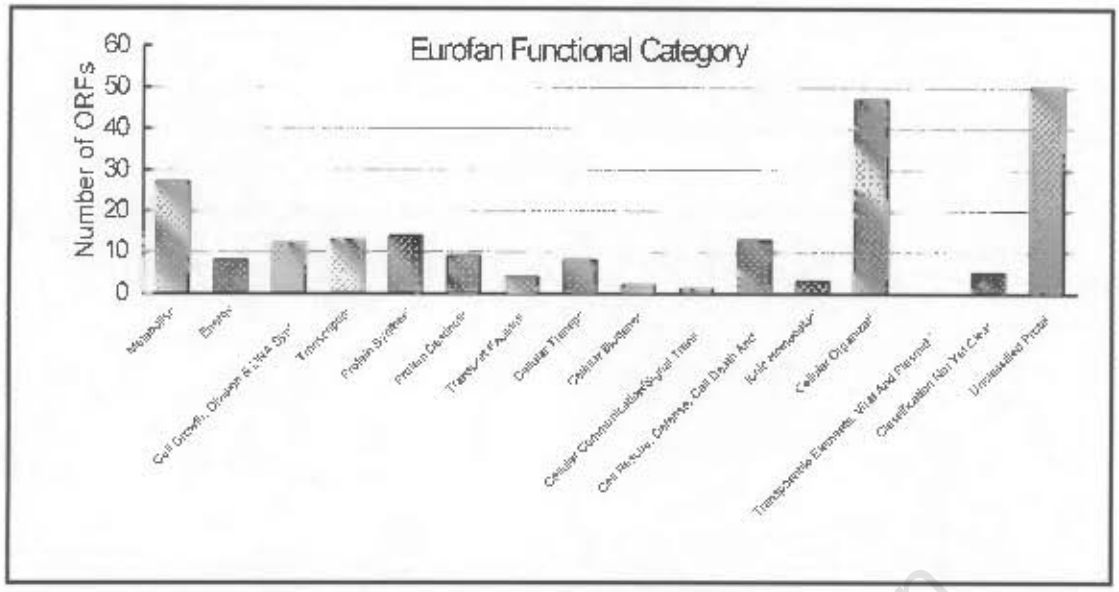

Figure 5.6 The number of genes affected according to Eurofan functional groups (1h).

The bar-graph shows the number of genes in each functional category affected by the deletion of *HHO1* at the 1h into lag phase (1h), after a 4°C incubation. The number of genes is plotted on the y-axis.

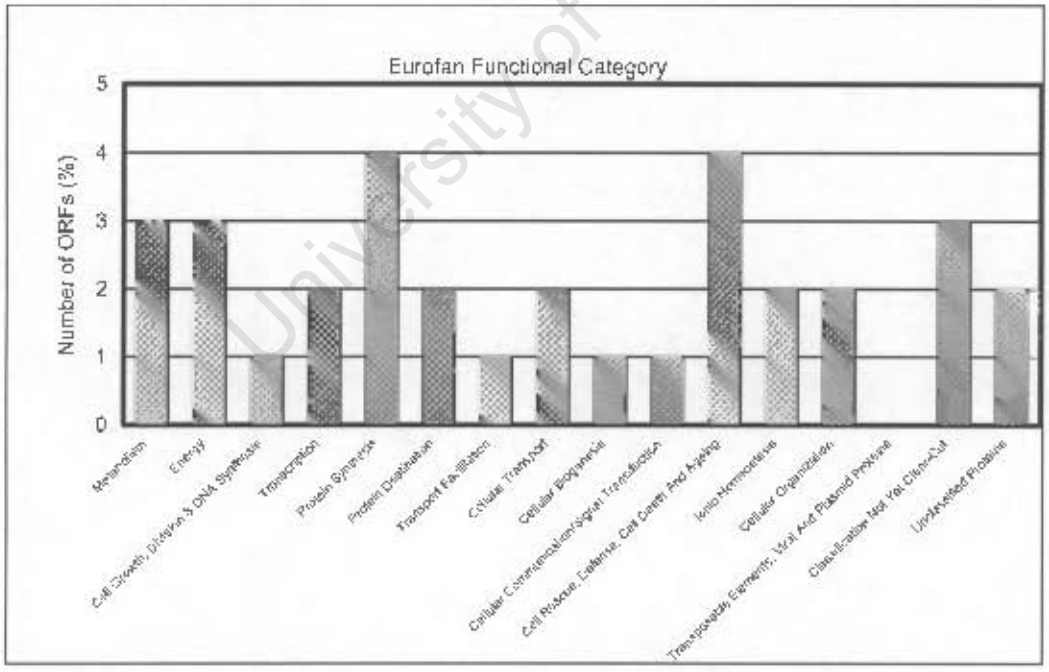

Figure 5.7 The percentage of genes affected according to Eurofan functional groups (1h). The bar-graph shows the % of genes in each functional category affected by the deletion of *HHO1* at the 1h into lag phase (0h), after a 4°C incubation. The % of genes is plotted on the y-axis.

The chromosomal analysis of the location of the genes affected by the absence of *HHO1*, shows that on chromosome IV and VII (Figure 5.8), the genes are confined, in part, to certain areas of the chromosome. The number of genes in these clusters have decreased at the 1h time point. The actual genes affected between the 0h and 1h time-points differ completely, though genes in the same regions are affected.

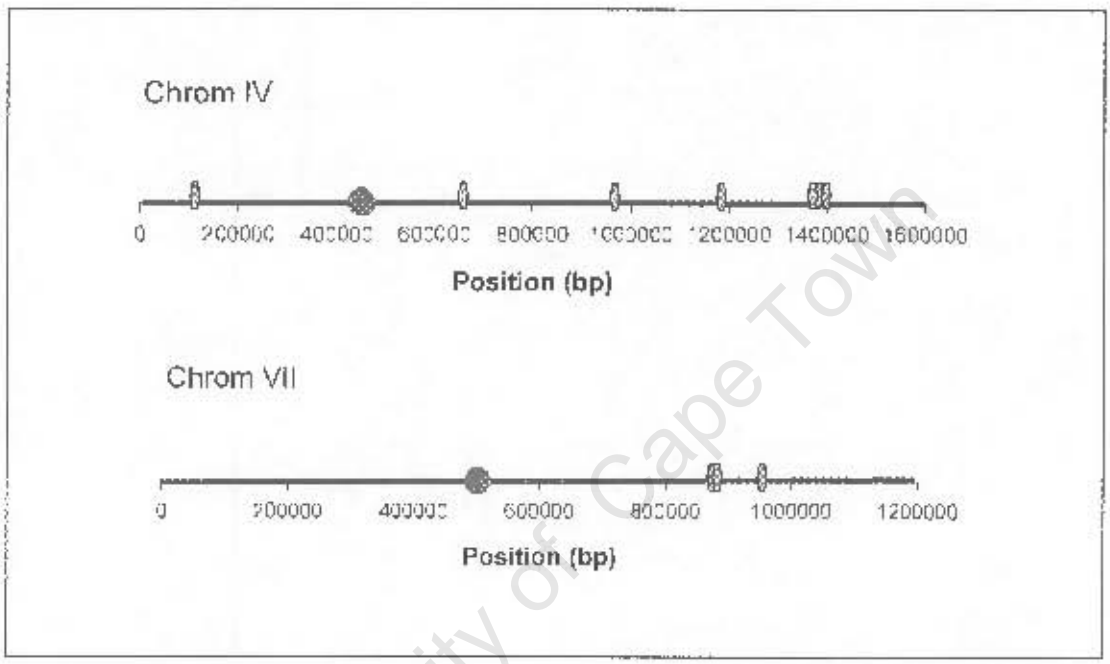

Figure 5.8 Clusters of genes affected by the absence of *HHO1* one hour into lag phase. Genes are indicated by the coloured diamonds. Centromeres are indicated by the maroon dots. Chromosome length bp is indicated.

5.5 Stationary Phase Microarray

Finally, a microarray experiment determining the differences in gene expression during the stationary phase of yeast growth, was performed.

During the stationary phase gene expression in WT cells is greatly diminished. It is therefore not surprising to find that only a small number of genes were affected by the absence of Hho1p. A total of 12 genes were down-regulated more than 2 × in the

hho1⁻ strain (Table 4). No genes were upregulated in the *hho1*⁻ strain during the stationary phase, neither were any genes down-regulated by more than 3 ×.

Gene name	Function	Chr #	Fold repression stationary phase
SDH4	Succinate dehydrogenase	IV	-2.02
GYP7	GTPase activating protein	IV	-2.31
URP1	Part ribosome/protein biosynthesis	II	-2.10
YBL086C	Unknown	II	-2.19
CDC19	Pyruvate kinase	I	-2.05
SUP46	Part ribosome/protein biosynthesis	II	-2.09
YBL092W	Part ribosome/protein biosynthesis	II	-2.55
HSP26	Heat shock protein/stress	II	-2.15
YDR134C	Unknown (similar to flo1p/5p/9p)	IV	-2.55
URP2	Part ribosome/protein biosynthesis	VIII	-2.35
RPB7	RNA pol II. DNA directed RNA pol	IV	-2.12
HSP42	Heatshock/stress	IV	-2.78
FUN19	Unknown	IV	-2.37
YDR133C	Unknown	I	-2.05

Table 4. Genes affected by the absence of *HHO1* during stationary phase.

The genes affected during stationary phase are listed above. The chromosome number, function and the expression ratio are also listed.

Contrary to what had been seen in Figure 5.2 and 5.3, here the genes were restricted to certain classes, evident in Table 4. Only genes that were responsible for metabolic processes or protein synthesis were affected. Mapping the genes according to their chromosomal location also revealed that the genes affected were not confined to

restricted regions of the chromosomes affected. Table 5 lists the number of genes affected on each chromosome.

Chr #	Chr Length	# genes affected
I	230203	2
II	813139	5
IV	1531929	6
VIII	562639	1

Table 5. Number of genes affected on chromosomes affected during stationary phase in absence of *HHO1*.

5.5 Verification of microarray data

The histone group of genes are expressed in the same pattern, during the cell cycle i.e. (Spellman *et al.*, 1998). The lag phase expression of histone H2A and H4 was therefore compared to the expression level of *HHO1* during the lag phase, in order to investigate the expression pattern of essential genes, which are also needed for DNA packaging.

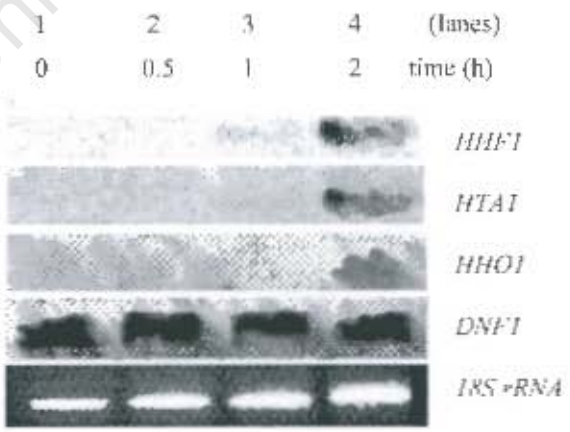

Figure 5.9. Northern blot of H2A (HTA1) and H4 (HHF1) gene transcripts during the lag phase. RNA was extracted at intervals during the lag phase following a 24 h 4°C incubation and probed for the presence of *HHF1* and *HTA1* mRNA. The *DNF1* was used as a constitutive expression control, while the 18S rRNA band was used as a loading control. 0h refers to RNA at the start of lag phase after the 4°C incubation; Samples were also taken 0.5h, 1h and 2h after the start of lag phase.

Similar to *HHO1*, H2A and H4 do not exhibit any mRNA transcript at 0 and 0.5h after the start of lag phase (Figure 5.9 lanes 1 and 2). However, mRNA is present in H2A and H4 at 1h (lane 3), while none is present in *HHO1*. All the histones show the presence of mRNA at 2h after the start of lag phase (lane 4). *DNF1,* the control for intact mRNA was expressed at all time points.

5.6 Summary

Microarray analyses were used to determine the differences in gene expression during lag phase and stationary phase in the *hho1*$^-$ strain. At the 0h time point 118 genes were up- and down-regulated in the *hho1*$^-$ strain. The genes affected were dispersed throughout the genome; however on chromosomes IV and VII the genes affected were clustered in certain regions of the chromosomes. Interestingly, the larger clustered region on vhromosome IV only showed upregulation of genes in the absence of *HHO1* at the 0h lag time point. At the 1h time point 218 genes were up- and down-regulated in the *hho1*$^-$ strain. Again, the genes affected on chromosomes IV and VII, were clustered in certain regions of the chromosomes, however, none of the genes affected at this time point matched those at the previous time point. During stationary phase, however, only 12 genes were affected in the *hho1*$^-$ strain. All these genes were down-regulated. The genes were not restricted to any particular chromosome, though only genes responsible for metabolic processes and protein synthesis were affected by the absence of Hho1p. No genes were down-regulated by more than 3 ×.

CHAPTER 6: DISCUSSION

6.1 Introduction

In this study we have addressed aspects of the biological role of Hho1p in *Saccharomyces cerevisiae*. It was already known that the deletion of *HHO1* in yeast had little effect on telomeric silencing, basal transcription or gene activation at a distance (Patterton *et al.*, 1998; Escher and Schaffner, 1997). Moreover, the *HHO1* deleted strain did not have an altered nucleosome repeat length (Patterton et al., 1998). It was suggested that the *hho1*$^-$ phenotype would become apparent if the cells were exposed to "sub-optimal conditions of a natural environment" (Patterton *et al.*, 1998). In this study, we have investigated the response of an *hho1*$^-$ strain to conditions of stress.

6.2 Phenotypic characterisation

We have shown that *hho1*$^-$ strains are more sensitive to DNA γ-irradiation, most likely because more double-strand DNA breaks are accumulated or alternatively, that one or both of the DNA repair pathways (homologous recombination or non-homologous end-joining) is less efficient in the absence of Hho1p. It was previously shown that chromatin structure impacted on DNA repair (reviewed by Game, 2000). It was also shown that linker histone H1 became transiently dephosphorylated after ionizing radiation (Guo *et al.*, 2000), and that dephosphorylation of histone H1 occured during apoptosis (Talasz *et al.*, 2002). These responses suggest that Hho1p plays a role in the mechanisms involved in DNA repair following damage induced by radiation. The exact mechanistic role is not currently understood.

Previous studies in the tomato plant have shown that levels of H1 increased in leaves exposed to water-deficit stress (Chao *et al.*, 1999; Scippa *et al.*, 2000). It is likely that the plant responds to the water stress condition by decreasing the number of genes expressed to only those required to survive the water stress condition. Genes that are shut down are likely incorporated into condensed chromatin structures that require the histone H1. We have found that *hho1*$^-$ strains are not more sensitive to either osmotic or oxidative stress (4.3). Although these stressed conditions are not identical to water-deficit stress, we have found that H1 is not required by the yeast cell to survive such related stress conditions.

It was shown in *Ascobolus* that H1 deletion strains have a decreased lifespan (Barra *et al.*, 2000). Genes responsible for early cell death are probably improperly regulated, causing the decreased lifespan. However, lifespan analyses in this study (4.5) have shown that the longevity of yeast cells is unaffected.

Interestingly, *HHO1* mRNA is expressed during the stationary phase (4.4). Yeast cells enter into the stationary phase in response to unfavourable conditions eg. starvation (reviewed by Werner-Washburne *et al.*, 1993). Cells can return to cell cycle and resume normal growth under favourable conditions. Stationary phase chromatin is characterised by being more tightly compacted compared to log phase chromatin (Lohr and Ide, 1979). The presence of *HHO1* mRNA during the stationary phase, hints at a role for Hho1p during stationary phase. Since starvation is another form of stress the cell encounters, Hho1p could perform a protective role for the cell, protecting it from damage, by shutting down all but the genes responsible for survival during stationary phase. The histone could bind to the promoters of genes, causing the

genes to be switched off. It is unclear whether the levels of Hho1p increase globally during stationary phase, or whether binding is localised to specific regions of the genome. A localised binding of Hho1p could form chromatin structures that encourage fast activation of genes when conditions become more favourable for growth.

The major phenotype identified in this study is cold-sensitivity (4.6). This phenotype seems to be linked to the stationary phase, as it is a prerequisite for *hho1*$^-$cells to have reached stationary phase growth, before they are subjected to 4°C, for the slow growth phenotype to be observed. It is possible that Hho1p is deposited during stationary phase in a way that enables genes to be activated quickly during lag phase. The chromatin in *hho1*$^-$ cells is not packaged in the same way during the stationary phase and therefore, the genes take a longer time to be activated when they exit stationary phase and enter into the lag phase. The microanalyses performed in this study, provide some evidence for a function for Hho1p in the stationary phase.

6.3 Microarray

Histone H1 has been implicated as a general repressor of transcriptional regulation (Section 1.6.1). However, this does not seem to be the case in *S. cerevisiae*. Whole genome microarray analysis with an *hho1*$^-$ strain showed a greater than two-fold decreased expression of only 27 genes (Hellauer *et al.*, 2001) in log phase cells, and it was shown in earlier studies that Hho1p did not act as a general repressor of gene expression (Escher and Schaffner, 1997), nor was basal transcription affected (Patterton *et al.*, 1998). Hho1p could therefore act by regulating only a subset of genes, as seen in *Tetrahymena* (Section 1.6.1).

Our microarray study (Chapter 5) suggests that Hho1p might be involved in playing a structural role in the genome. During stationary phase, when the genome is effectively "switched off" Hho1p might be deposited, forming certain structures that enable speedy activation when favourable conditions return. This hypothesis is supported by a recent study by Ali and Thomas (Ali, 2001), that demonstrated that Hho1p was localised throughout the yeast genome.

The differences in gene expression in *hho1*⁻ strains, seen in the clustered regions of chromosomes IV and VII during the lag phase, could therefore suggest regions of localised chromosome structure, formed by the presence of Hho1p. The genes affected at the 0h and 1h time points are not the same, though the genes affected do occur in the same regions of the chromosomes (5.2 and 5.3). It is interesting that the genes in these regions are both up- and down-regulated. Therefore the presence of Hho1p is needed to activate some genes. It is possible that phosphorylation of Hho1p enables decondensation of the chromatin fibres, enabling transcription factors and other activators to bind. However, some effects might be indirect e.g. through the activation of a gene for a transcriptional repressor.

Chromatin-immunoprecipitation assays will need to be performed to investigate the physical presence of H1 at the identified clusters. In addition, microarray analysis of the expression pattern at numerous time points at the start of the lag phase would be very informative regarding the dynamic nature and distribution of H1 during these entry gene activation events.

6.4 Future work

Questions remain regarding the lag phase cold sensitive phenotype. Since *HHO1* mRNA is not present during the lag phase, it is essential to establish at which level Hho1p is present during the lag phase. This will show whether Hho1p is deposited during the stationary phase and plays a role during the lag phase.

Furthermore, the clustered regions of chromosomes IV and VII should be examined in detail. Chromatin-immunoprecipitation assays will show whether Hho1p occurs at the promoters of the genes affected in these regions. DNase I digestion of these promoters should also establish whether these promoters have an H1-dependent structure. These experiments are planned for the immediate future.

REFERENCES

Aboussekhra, A., Vialard, J.E., Morrison, D.E., de la Torre-Ruiz, M.A., Cernakova, L., Fabre, F., Lowndes, N.F. (1996) A novel role for the budding yeast RAD9 checkpoint gene in DNA damage-dependent transcription. EMBO J. 15, 3912-3922.

Adams, A., Gottschling, D.E., Kaiser, C.A., Stearns, T. (1998) Methods in Yeast Genetics: A Cold Spring Harbor Laboratory Course Manual. Cold Spring Harbor Laboratory Press, Plainview, New York.

Ali, T. (2001) Characterisation of Hho1p, the putative *Saccharomyces cerevisiae.* Department of Biochemistry. University of Cambridge. Cambridge.

Allan, J., Cowling, G.J., Harborne, N., Cattini, P., Craigie, R., Gould, H. (1981) Regulation of the higher-order structure of chromatin by histones H1 and H5. J Cell Biol. 90, 279-85.

Aoyagi, S., Narlikar, G., Zheng, C., Sif, S., Kingston, R.E., Hayes, J.J. (2002) Nucleosome remodeling by the human SWI/SNF complex requires transient global disruption of histone-DNA interactions. Mol Cell Biol. 22, 3653-62.

Archer, T.K., Lefebvre, P., Wolford, R.G., Hager, G.L. (1992) Transcription factor loading on the MMTV promoter: a bimodal mechanism for promoter activation. Science 255, 1573-6.

Ascenzi, R., Gantt, J.S. (1999) Subnuclear distribution of the entire complement of linker histone variants in Arabidopsis thaliana. Chromosoma 108, 345-355.

Ausio, J. (2000) Are linker histones (histone H1) dispensable for survival? Bioessays 22, 873-7.

Ausubel, F., Brent, R., Kingston, R.E., Moore, D.D., Seidman, J.G., Smith, J.A., Struhl, K. (1995) Short Protocols in Molecular Biology. John Wiley & Sons, Inc, Boston.

Baneyx, F. (1999) Recombinant protein expression in *Escherichia coli*. Opin. Biotechnol. 10, 411-21.

Barra, J.L., Rhounim, L., Rossignol, J.L., Faugeron, G. (2000) Histone H1 is dispensable for methylation-associated gene silencing in Ascobolus immersus and essential for long life span. Mol Cell Biol. 20, 61-69.

Baxevanis, A.D., Landsman, D. (1998) Homology model building of Hho1p supports its role as a yeast histone H1 protein. In Silico Biol. 1, 5-11.

Becker, D.M., Guarente, L. (1991) High-efficiency transformation of yeast by electroporation. Methods Enzymol., 194.

Bednar, J., Horowitz, R.A., Grigoryev, S.A., Carruthers, L.M., Hansen, J.C., Koster, A.J., Woodcock, C.L. (1998) Nucleosomes, linker DNA, and linker histone form a unique structural motif that directs the higher-order folding and compaction of chromatin. Proc Natl Acad Sci U S A. 95, 14173-8.

Bedoyan, J.K., Lejnine, S., Makarov, V.L., Langmore, J.P. (1996) Condensation of rat telomere-specific nucleosomal arrays containing unusually short DNA repeats and histone H1. J Biol Chem. 271, 18485-18493.

Bleher, R., Martin, R. (1999) Nucleo-cytoplasmic translocation of histone H1 during the HeLa cell cycle. Chromosoma 108, 308-316.

Bohm, L., Crane-Robinson, C. (1984) Proteases as structural probes for chromatin: the domain structure of histones. Biosci Rep. 4. 365-86.

Bouvet, P., Dimitrov, S., Wolffe, A.P. (1994) Specific regulation of Xenopus chromosomal 5S rRNA gene transcription in vivo by histone H1. Genes Dev. 8, 1147-59.

Bradbury, E.M., Inglis, R.J.,Matthews, H.R. (1974) Control of cell division by very rich lysine rich histone (F1) phosphorylation. Nature (London) 247, 257-61.

Bradbury, E.M. (1992) Reversible Histone Modifications and the Chromosome Cell Cycle. Bioessays 14, 9-16.

Brocard, M.P., Triebe, S., Peretti, M., Doenecke, D., Khochbin S. (1997) Characterization of the two H1(zero)-encoding genes from Xenopus laevis. Gene 189, 127-134.

Chao, W.S., Gu, Y.Q., Pautot, V. V., Bray, E.A., Walling, L.L. (1999) Leucine aminopeptidase RNAs, proteins, and activities increase in response to water deficit, salinity, and the wound signals systemin, methyl jasmonate, and abscisic acid. Plant Physiol. 120, 979-92.

Cherry, J.M., Ball, C., Weng, S., Juvik, G., Schmidt, R., Adler, C., Dunn, B., Dwight, S., Riles, L., Mortimer, R.K., Botstein, D. (1997) Genetic and physical maps of Saccharomyces cerevisiae. Nature 387, 67-73.

Cho, R.J., Campbell, M.J., Winzeler, E.A., Steinmetz, L., Conway, A., Wodicka, L., Wolfsberg, T.G., Gabrielian, A.E., Landsman, D., Lockart, D.J. and Davis, R.W. (1998) A genome-wide transcriptional analysis of the mitotic cell cycle. Mol Cell, 2, 65-73.

Cirillo, L.A., McPherson, C.E., Bossard, P., Stevens, K., Cherian, S., Shim, E.Y., Clark, K.L., Burley, S.K., Zaret, K.S. (1998) Binding of the winged-helix transcription factor HNF3 to a linker histone site on the nucleosome. EMBO J. 17, 244-254.

Clark, D.J., Kimura, T. (1990) Electrostatic mechanism of chromatin folding. J Mol Biol. 211, 883-996.

Clauser, K.R., Baker, P., Burlingame, A.L. (1999) Role of accurate mass measurement (+/- 10 ppm) in protein identification strategies employing MS or MS/MS and database searching. Anal Chem. 71, 2871-82.

Cole, R.D. (1984) A minireview of microheterogeneity in H1 histone and its possible significance. Anal Biochem. 136. 24-30.

Dasso, M., Dimitrov, S., Wolffe, A.P. (1994) Nuclear assembly is independent of linker histones. Proc Natl Acad Sci U S A. 91, 12477-81.

Davie, J.R., Saunders, C.A, Walsh, J.M., Weber, S.C. (1981) Histone modifications in the yeast S. Cerevisiae. Nucleic Acids Res. 9, 3205-16.

Davie, J.R., Chadee, D.N. (1998) Regulation and regulatory parameters of histone modifications. J Cell Biochem Suppl. 30-31, 203-13.

De Lange, R.J., Farnbrough, D.M., Smith, E.L., and Bonner, J. (1969) Calf and pea histone IV: the complete amino acid sequence of calf thymus histone IV; presence of N-acetyllysine. J Biol Chem. 244, 319-334.

DeRisi, J.L., Iyer, V.R., Brown, P.O. (1997) Exploring the metabolic and genetic control of gene expression on a genomic scale. Science 278, 680-6.

Dimitrov, S., Almouzni, G., Dasso, M., Wolffe, A.P. (1993) Chromatin transitions during early Xenopus embryogenesis: changes in histone H4 acetylation and in linker histone type. Dev Biol. 160, 214-27.

Dou, Y., Gorovsky, M.A. (2000) Phosphorylation of linker histone H1 regulates gene expression in vivo by creating a charge patch. Mol Cell. 6, 225-31.

Dou, Y., Gorovsky, M.A. (2002) Regulation of transcription by H1 phosphorylation in Tetrahymena is position independent and requires clustered sites. Proc Natl Acad Sci U S A. 99, 6142-46.

Engelke, D.R., Ng, S.Y., Shastry, B.S., Roeder, R.G. (1980) Specific interaction of a purified transcription factor with an internal control region of 5S RNA genes. Cell 19, 717-28.

Escher, D., Schaffner, W. (1997) Gene activation at a distance and telomeric silencing are not affected by yeast histone H1. Mol Gen Genet. 256, 456-61.

Estruch, F. (2000) Stress-controlled transcription factors, stress-induced genes and stress tolerance in budding yeast. FEMS Microbiol Rev. 24, 469-86.

Fan, Y., Sirotkin, A., Russell, R.G., Ayala, J., Skoultchi, A.I. (2001) Individual somatic H1 subtypes are dispensable for mouse development even in mice lacking the H1(0) replacement subtype. Mol Cell Biol. 21, 7933-7943.

Freidkin, I., Katcoff, D.J. (2001) Specific distribution of the Saccharomyces cerevisiae linker histone homolog HHO1p in the chromatin. Nucleic Acids Res. 29, 4043-51.

Game, J.C. (2000) The Saccharomyces repair genes at the end of the century. Mutat. Res. 451, 277-293.

Garcia-Ramirez, M., Rocchini, C., Ausio, J. (1995) Modulation of chromatin folding by histone acetylation. J Biol Chem. 270, 17923-28.

Garrard, W.T. (1991) Histone H1 and the conformation of transcriptionally active chromatin. Bioessays. 13, 87-8.

Goffeau, A., Barrell, B.G., Bussey,H., Davis, R.W., Dujon, B., Feldmann, H., Galibert, F., Hoheisel, J.D., Jacq, C., Johnston, M., Louis, E.J., Mewes, H.W., Murakami, Y., Philippsen, P., Tettelin, H., Oliver, S.G. (1996) Life with 6000 genes. Science 274, 563-7.

Gorovsky, M.A. (1973) Macro- and micronuclei of Tetrahymena pyriformis: a model system for studying the structure and function of eukaryotic nuclei. J Protozool. 20, 19-25.

Goytisolo, F.A., Gerchman, S.E., Yu, X., Rees, C., Graziano, V., Ramakrishnan, V., Thomas, J.O. (1996) Identification of two DNA-binding sites on the globular domain of histone H5. EMBO J. 15, 3421-3429.

Grunstein, M. (1997) Histone acetylation in chromatin structure and transcription. Nature 389, 349-352.

Grunwald, D., Lawrence, J.J., Khochbin, S. (1995) Accumulation of histone H1(0) during early Xenopus laevis development. Exp Cell Res. 218, 586-95.

Gunjan, A., Sittman, D.B., Brown, D.T. (2001) Core histone acetylation is regulated by linker histone stoichiometry in vivo. J Biol Chem. 276, 3635-40.

Guo, C.Y., Mizzen, C., Wang, Y., Larner, J.M. (2000) Histone H1 and H3 dephosphorylation are differentially regulated by radiation-induced signal transduction pathways. Cancer Res. 60, 5667-72.

Hansen, J.C., Tse, C., Wolffe, A.P. (1998) Structure and function of the core histone N-termini: more than meets the eye. Biochemistry 37, 17637-41.

Harrison, G.S., Findly, R.C., Karrer, K.M. (1986) Site-specific methylation of adenine in the nuclear genome of a eukaryote, Tetrahymena thermophila. Mol Cell Biol. 6, 2364-70.

Hellauer, K., Sirard, E., Turcotte, B. (2001) Decreased expression of specific genes in yeast cells lacking histone H1. J Biol Chem. 276, 13587-92.

Herrera, J.E., Sakaguchi, K., Bergel, M., Trieschmann, L., Nakatani, Y., Bustin, M. (1999) Specific acetylation of chromosomal protein HMG-17 by PCAF alters its interaction with nucleosomes. Mol Cell Biol. 19, 3466-73.

Heussen, C., Nackerdien, Z., Smit, B.J., Bohm,L. (1987) Irradiation damage in chromatin isolated from V-79 Chinese hamster lung fibroblasts. Radiat Res. 110, 107-13.

Hill, C.S., Rimmer, J.M., Green, B.N., Finch, J.T., Thomas, J.O. (1991) Histone-DNA interactions and their modulation by phosphorylation of -Ser-Pro-X-Lys/Arg- motifs. EMBO J. 10, 1939-48.

Hill, D.A., Imbalzano, A.N. (2000) Human SWI/SNF nucleosome remodeling activity is partially inhibited by linker histone H1. Biochemistry. 39, 11649-11656.

Holstege, F.C., Jennings, E.G., Wyrick, J.J., Lee ,T.I., Hengartner, C.J., Green, M.R., Golub, T.R., Lander, E.S., Young, R.A. (1998) Dissecting the regulatory circuitry of a eukaryotic genome. Cell 95, 717-28.

Karrer, K.M., VanNuland, T.A. (2002) Methylation of adenine in the nuclear DNA of Tetrahymena is internucleosomal and independent of histone H1. Nucleic Acids Res. 30, 1364-1370.

Kennedy, B.K., Austriaco, N.R., Zhang, J., Guarente, L. (1995) Mutation in the silencing gene SIR4 can delay aging in S. cerevisiae. Cell 80, 485-96.

Khochbin, S., Wolffe, A.P. (1994) Developmentally regulated expression of linker-histone variants in vertebrates. Eur J Biochem. 225, 501-10.

Klug, A., Rhodes, D., Smith, J., Finch, J.T., Thomas, J.O. (1980) A low resolution structure for the histone core of the nucleosome. Nature 287, 509-16.

Kornberg, R. (1974) Chromatin structure: a repeating unit of histones and DNA. Science 184, 868-71.

Kornberg, R.D., Lorch, Y. (1999) Twenty-five years of the nucleosome, fundamental particle of the eukaryote chromosome. Cell 98, 285-294.

Laemmli, U.K. (1970) Cleavage of structural proteins during the assembly of the head of bacteriophage T4. Nature 227, 680-5.

Landsman, D. (1996) Histone H1 in Saccharomyces cerevisiae: a double mystery solved? Trends Biochem Sci. 21, 287-8.

Lee, H.L., Archer, T.K. (1994) Nucleosome-mediated disruption of transcription factor-chromatin initiation complexes at the mouse mammary tumor virus long terminal repeat in vivo. Mol Cell Biol. 14, 32-41.

Lee, K.M., Hayes, J.J. (1997) The N-terminal tail of histone H2A binds to two distinct sites within the nucleosome core. Proc Natl Acad Sci U S A. 94, 8959-64.

Lee, H.L., Archer, T.K. (1998) Prolonged glucocorticoid exposure dephosphorylates histone H1 and inactivates the MMTV promoter. EMBO J. 17, 1454-66.

Lever, M.A., Th'ng, J.P., Sun, X., Hendzel, M.J. (2000) Rapid exchange of histone H1.1 on chromatin in living human cells. Nature 408, 873-876.

Lin, Q., Sirotkin, A., Skoultchi, A.I. (2000) Normal spermatogenesis in mice lacking the testis-specific linker histone H1t. Mol Cell Biol. 20, 2122-28.

Lohr, D., Van Holde, K.E. (1975) Yeast chromatin subunit structure. Science 188, 165-6.

Lohr, D., Ide, G. (1979) Comparison on the structure and transcriptional capability of growing phase and stationary yeast chromatin: a model for reversible gene activation. Nucleic Acids Res. 6, 1909-27.

Lu, Z.H., Sitman, D.B., Romanowski, P., Leno, G.H. (1998) Histone H1 Reduces the Frequency of initiation in Xenopus Egg Extract by Limiting the Assembly of Pre-replication complexes on Sperm Chromatin. Mol Biol. Cell 9, 1163-1176.

Luger, K., Mader, A.W., Richmond,R.K., Sargent, D.F., Richmond, T.J. (1997) Crystal structure of the nucleosome core particle at 2.8 A resolution. Nature 389, 251-260.

Makarov, V.L., Lejnine, S., Bedoyan, J., Langmore, J.P. (1993) Nucleosomal organization of telomere-specific chromatin in rat. Cell 73, 775-87.

Marc, P., Devaux, F., Jacq, C. (2001) yMGV: an online tool for rapid visualisation of published genome-wide yeast expression data. Nucleic Acid Res. 29, E63-3.

Mewes, H.W., Albermann, K., Heumann, K., Liebl, S., Pfeiffer, F. (1997) MIPS: a database for protein sequences, homology data and yeast genome information. Nucl. Acids Res. 25, 28-30.

Misteli, T., Gunjan, A., Hock, R., Bustin, M., Brown, D.T. (2000) Dynamic binding of histone H1 to chromatin in living cells. Nature 408, 877-81.

Mizzen, C.A., Dou, Y., Liu, Y., Cook, R.G., Gorovsky, M.A., Allis, C.D. (1999) Identification and mutation of phosphorylation sites in a linker histone. Phosphorylation of macronuclear H1 is not essential for viability in tetrahymena. J Biol Chem. 274, 14533-6.

Ner, S.S., Travers, A.A. (1994) HMG-D, the Drosophila melanogaster homologue of HMG 1 protein, is associated with early embryonic chromatin in the absence of histone H1. EMBO J. 13, 1817-22.

Newport, J., Kirschner, M. (1982) A major developmental transition in early Xenopus embryos: I. characterization and timing of cellular changes at the midblastula stage. Cell. 30, 675-86.

Nickel, B.E., Davie, J.R. (1987) Structure of polyubiquitinated histone H2A. Biochemistry. 28, 964-8.

Nightingale, K., Wolffe, A.P. (1995) Methylation at CpG sequences does not influence histone H1 binding to a nucleosome including a Xenopus borealis 5S rRNA gene. J. Biol. Chem. 270, 4197-200.

Nightingale, K., Dimitrov, S., Reeves, R., Wolffe, A.P. (1996) Evidence for a shared structural role for HMG1 and linker histones B4 and H1 in organizing chromatin. EMBO J. 15, 548-61.

Ohsumi, K., Katagiri, C. (1991) Occurrence of H1 subtypes specific to pronuclei and cleavage-stage cell nuclei of anuran amphibians. Dev. Biol. 147, 110-120.

Padilla, P.A., Fuge, E.K., Crawford, M.E., Errett, A., Werner-Washburne, M. (1998) The highly conserved, coregulated SNO and SNZ gene families in Saccharomyces cerevisiae respond to nutrient limitation. J Bacteriol. 180, 5718-26.

Panetta, G., Buttinelli, M., Flaus, A., Richmond, T.J., Rhodes, D. (1998) Differential nucleosome positioning on Xenopus oocyte and somatic 5 S RNA genes determines both TFIIIA and H1 binding: a mechanism for selective H1 repression. J Mol Biol. 282, 683-97.

Patterton, H.G., Landel, C.C., Landsman, D., Peterson, C.L., Simpson, R.T. (1998) The biochemical and phenotypic characterization of Hho1p, the putative linker histone H1 of Saccharomyces cerevisiae. J Biol Chem. 273, 7268-7276.

Pennings, S., Meersseman, G., Bradbury, E.M. (1994) Linker histones H1 and H5 prevent the mobility of positioned nucleosomes. Proc Natl Acad Sci U S A. 91, 10275-9.

Perry, C.A., Annunziato, A.T. (1989) Influence of histone acetylation on the solubility, H1 content and DNase I sensitivity of newly assembled chromatin. Nucleic Acids Res. 17, 4275-91.

Peterson, R.C., Doering, J.L., Brown, D.D. (1980) Characterization of two xenopus somatic 5S DNAs and one minor oocyte-specific 5S DNA. Cell 20, 131-41.

Pham, A.D., Sauer, F. (2000) Ubiquitin-activating/conjugating activity of TAFII250, a mediator of activation of gene expression in Drosophila. Science 289, 2357-60.

Poccia, D.L. (1986) Remodelling of nucleoproteins during gametogenesis, fertilisation and early development. Int. Rev. Cytol. 105, 1-65.

Pruss, D., Bartholomew, B., Persinger, J., Hayes, J., Arents, G., Moudrianakis, E.N., Wolffe, A.P. (1996) An asymmetric model for the nucleosome: a binding site for linker histones inside the DNA gyres. Science 274, 614-17.

Prymakowska-Bosak, M., Przewloka, M.R., Iwkiewicz, J., Egierszdorff, S., Kuras, M., Chaubet, N., Gigot, C., Spiker, S., Jerzmanowski, A. (1996) Histone H1 overexpressed to high level in tobacco affects certain developmental programs but has limited effect on basal cellular functions. Proc Natl Acad Sci U S A. 93, 10250-55.

Prymakowska-Bosak, M., Przewloka, M.R., Slusarczyk, J., Kuras, M., Lichota, J., Kilianczyk, B., Jerzmanowski, A. (1999) Linker histones play a role in male meiosis and the development of pollen grains in tobacco. Plant Cell. 11, 2317-29.

Rajpal, D.K., Wu, X., Wang, Z. (2000) Alteration of ultraviolet-induced mutagenesis in yeast through molecular modulation of the REV3 and REV7 gene expression. Mutat Res. 461, 133-43.

Ramakrishnan, V., Finch, J.T., Graziano, V., Lee, P.L., Sweet, R.M. (1993) Crystal structure of globular domain of histone H5 and its implications for nucleosome binding. Nature 362, 219-233.

Ramon, A., Muro-Pastor, M., Scazzocchio, C., Gonzalez, R. (2000) Deletion of the unique gene encoding a typical histone H1 has no apparent phenotype in Aspergillus nidulans. Mol Microbiol. 35, 223-233.

Richard-Foy, H., Hager, G.L. (1987) Sequence-specific positioning of nucleosomes over the steroid-inducible MMTV promoter. EMBO J. 6, 2321-8.

Roth, S.Y., Allis, C.D. (1992) Chromatin condensation: does histone H1 dephosphorylation play a role? Trends Biochem Sci. 17, 93-8.

Roth, F.P., Hughes, J.D., Estep, P.W., Church, G.M. (1998) Finding DNA regulatory motifs within unaligned noncoding sequences clustered by whole-genome mRNA quantification. Nat Biotechnol. 16, 939-45.

Schlissel, M.S., Brown, D.D. (1984) The transcriptional regulation of Xenopus 5S genes in chromatin: the roles of active stable transcription complexes and histone H1. Cell 37, 903-11.

Scippa, G.S., Griffiths, A., Chiatante, D., Bray, E.A. (2000) The H1 histone variant of tomato, H1-S, is targeted to the nucleus and accumulates in chromatin in response to water-deficit stress. Planta 211, 173-181.

Sera, T., Wolffe, A.P. (1998) Role of histone H1 as an architectural determinant of chromatin structure and as a specific repressor of transcription on Xenopus oocyte 5S rRNA genes. Mol Cell Biol. 18, 3668-3680.

Shen, X., Yu, L., Weir, J.W., Gorovsky, M.A. (1995) Linker histones are not essential and affect chromatin condensation in vivo. Cell 82, 47-56.

Shen, X., Gorovsky, M.A. (1996) Linker histone H1 regulates specific gene expression but not global transcription in vivo. Cell 82, 475-83.

Shim, E.Y., Woodcock, C., Zaret, K.S. (1998) Nucleosome positioning by the winged helix transcription factor HNF3. Genes Dev. 12, 5-10.

Simpson, R.T. (1978) Structure of the chromatosome, a chromatin particle containing 160 base pairs of DNA and all the histones. Biochemistry 17, 5524-5531.

Smith, B.J., Harris, M.R., Sigournay, C.M., Mayes, E.L., Bustin, M. (1984) A survey of H1o-and H5-like protein structure and distribution in higher and lower eukaryotes. Eur J Biochem. 138, 309-17.

Spellman, P.T., Sherlock,G., Zhang, M.Q., Iyer, V.R., Anders, K., Eisen, M.B., Brown, P.O., Botstein, D., Futcher, B. (1998) Comprehensive identification of cell cycle-regulated genes of the yeast Saccharomyces cerevisiae by microarray hybridization. Mol Biol Cell. 9, 3273-97.

Spencer, V.A., Davie, J.R. (1999) Role of covalent modifications of histones in regulating gene expression. Gene 240, 1-12.

Srebreva, L., Zlatanova, J., Miloshev, G., Tsanev, R. (1987) Immunological evidence for the existence of H1-like histone in yeast. Eur J Biochem. 165, 449-54.

Strahl, B.D., Allis, C.D. (2000) The language of covalent histone modifications. Nature 403, 41-5.

Sulkowski, E. (1989) The saga of IMAC and MIT. Bioessays 10, 170-175.

Takami, Y., Nakayama, T. (1997) One allele of the major histone gene cluster is enough for cell proliferation of the DT40 chicken B cell line. Biochim Biophys Acta 1354, 105-15.

Talasz, H., Helliger, W., Sarg, B., Debbage, P.L., Puschendorf, B., Lindner, H. (2002) Hyperphosphorylation of histone H2A.X and dephosphorylation of histone H1 subtypes in the course of apoptosis. Cell Death Differ. 9, 27-39.

Thoma, F., Koller, T., Klug, A. (1979) Involvement of histone H1 in the organization of the nucleosome and of the salt-dependent superstructures of chromatin. J Cell Biol. 83, 402-27.

Thomas, J.O., Rees, C. (1983) Exchange of histones H1 and H5 between chromatin fragments. A preference of H5 for higher-order structures. Eur J Biochem. 134, 109-15.

Thomas, J.O. (2000) Histone H1: location and role. Curr Opin Cell Biol. 11, 312-317.

Travers, A. (1999) The location of the linker histone on the nucleosome. Trends Biochem Sci. 24, 4-7.

Tsapali, D.S., Sekeri-Pataryas, K.E., Prombona, A., Sourlingas, T.G. (2000) mRNA levels of the linker histone variant, H1o, in mitotically active human diploid fibroblasts as a function of the phases of the cell cycle and cumulative population doublings. Mech Ageing Dev. 121, 101-112.

Tse, C., Hansen, J.C. (1997) Hybrid trypsinized nucleosomal arrays: identification of multiple functional roles of the H2A/H2B and H3/H4 N-termini in chromatin fiber compaction. Biochemistry. 36, 11381-8.

Ura, K., Wolffe, A.P., Hayes, J.J. (1994) Core histone acetylation does not block linker histone binding to a nucleosome including a Xenopus borealis 5 S rRNA gene. J Biol Chem. 269, 27171-4.

Ura, K., Hayes, J.J, Wolffe, A.P. (1995) A positive role for nucleosome mobility in the transcriptional activity of chromatin templates: restriction by linker histones. EMBO J. 14, 3752-65.

Ura, K., Nightingale, K., Wolffe, A.P. (1996) Differential association of HMG1 and linker histones B4 and H1 with dinucleosomal DNA: structural transitions and transcriptional repression. EMBO J. 15, 4959-69.

Usachenko, S.I., Gavin, I.M., Bavykin, S.G. (1996) Alterations in nucleosome core structure in linker histone-depleted chromatin. J Biol Chem. 271, 3831-6.

Ushinsky, S.C., Bussey, H., Ahmed, A.A., Wang, Y., Williams, B.A., Storms, R.K. (1997) Histone H1 in Saccharomyces cerevisiae. Yeast 13, 151-161.

Van Holde, K.E. (1989) Chromatin. Springer-Verlag, New York.

Vermaak, D., Steinbach, O.C., Dimitrov, S., Rupp, R.A., Wolffe, A.P. (1998) The globular domain of histone H1 is sufficient to direct specific gene repression in early Xenopus embryos. Curr Biol. 8, 533-6.

Vernet, G., Sala-Rovira, M., Maeder, M., Jacques, F., Herzog, M. (1990) Basic nuclear proteins of the histone-less eukaryote Crypthecodinium cohnii (Pyrrhophyta): two-dimensional electrophoresis and DNA-binding properties. Biochim Biophys Acta. 1048, 281-9.

Vignali, M., Hassan, A.H., Neely, K.E., Workman, J.L. (2000) ATP-dependent chromatin-remodeling complexes. Mol Cell Biol. 20, 1899-910.

Weintraub, H. (1985) Assembly and propagation of repressed and depressed chromosomal states. Cell 42, 705-11.

Weisman, R., Choder, M. (2001) The fission yeast TOR homolog, tor1+, is required for the response to starvation and other stresses via a conserved serine. J Biol Chem. 276, 7027-32.

Werner-Washburne, M., Braun, E., Johnston, G.C., Singer, R.A. (1993) Stationary phase in the yeast Saccharomyces cerevisiae. Microbiol Rev. 57, 383-401.

Wodicka, L., Dong, H., Mittmann, M., Ho, M.H., Lockhart, D.J. (1997) Genome-wide expression monitoring in Saccharomyces cerevisiae. Nat Biotechnol. 15, 1359-67.

Wolffe, A.P., Brown, D.D. (1987) Differential 5S RNA expression in vitro. Cell 51, 733-40.

Wolffe, A.P. (1989) Dominant and specific repression of Xenopus oocyte 5S RNA genes and satellite I DNA by histone H1. EMBO J. 8, 527-37.

Wolffe, A. (1994) Architectural transcription factors. Science 264, 1100-1.

Wolffe, A.P., Hayes, J.J. (1999) Chromatin disruption and modification. Nucleic Acids Res. 27, 711-20.

Wormington, W.M., Brown, D.D. (1983) Onset of 5S RNA gene regulation during Xenopus embryogenesis. Dev. Biol. 99, 248-57.

Wu, M., Allis, C.D., Richman, R., Cook, R.G., Govorsky, M.A. (1986) An intervening sequence in an unusual histone H1 gene of Tetrahymena thermophila. Proc. Natl Acad. Sci. USA 83, 8674-8.

Wu, J., Grunstein, M. (2000) 25 years after the nucleosome model: chromatin modifications. Trends Biochem Sci. 25, 619-623.

Zhou, Y.B., Gerchman, S.E., Ramakrishnan, V., Travers, A., Muyldermans, S. (1998) Position and orientation of the globular domain of linker histone H5 on the nucleosome. Nature 395, 402-405.

Zlatanova, J. (1990) Histone H1 and the regulation of transcription of eukaryotic genes. Trends Biochem Sci. 15, 273-76.

Zlatanova, J., Van Holde, K. (1992) Histone H1 and transcription: still an enigma? J Cell Sci. 103, 889-95.

Zlatanova, J., Leuba, S.H., van Holde, K. (1998) Chromatin fiber structure: morphology, molecular determinants, structural transitions. Biophys J. 74, 2554-66.